İSTANBUL TECHNICAL UNIVERSITY ★ INFORMATICS INSITUTE

COMPUTATIONAL BLOOD CLOTTING MODELLING WITH COUPLED LATTICE BOLTZMANN AND DISCRETE ELEMENT METHODS

M.Sc. Thesis by
Okan DOĞRU

Department : **Computational Science and Engineering**

Programme : **Computational Science and Engineering**

APRIL 2011

İSTANBUL TECHNICAL UNIVERSITY ★ INFORMATICS INSITUTE

COMPUTATIONAL BLOOD CLOTTING MODELLING WITH COUPLED LATTICE BOLTZMANN AND DISCRETE ELEMENT METHODS

M.Sc. Thesis by
Okan DOĞRU
(702081015)

Date of submission : **06 May 2011**
Date of defence examination : **08 June 2011**

Supervisor (Chairman) : **Prof. Dr. M. Serdar ÇELEBİ (İ.T.Ü.)**
Members of the Examining Committee : **Prof. Dr. Ömer GÖREN (İ.T.Ü.)**
Assist. Prof. Dr. Adem TEKİN (İ.T.Ü.)

APRIL 2011

İSTANBUL TEKNİK ÜNİVERSİTESİ ★ BİLİŞİM ENSTİTÜSÜ

LATTICE BOLTZMANN VE DISCRETE ELEMENT YÖNTEMLERİ KULLANILARAK KANIN PIHTILAŞMASININ MODELLENMESİ

YÜKSEK LİSANS TEZİ

Okan DOĞRU
(702081015)

Tezin Enstitüye Verildiği Tarih : **06 Mayıs 2011**
Tezin Savunulduğu Tarih : **08 Haziran 2011**

Tez Danışmanı : **Prof. Dr. M. Serdar ÇELEBİ (İ.T.Ü.)**
Diğer Jüri Üyeleri : **Prof. Dr. Ömer GÖREN (İ.T.Ü.)**
Yrd. Doç. Dr. Adem TEKİN (İ.T.Ü.)

NİSAN 2011

FOREWORD

This master thesis where written during the time-period from summer 2009 until spring 2011, under the teaching supervision of Prof. Dr. M. Serdar Çelebi, Informatics Institute, İstanbul Technical University.

I would like to thank Prof. Dr. M. Serdar Çelebi for being my advisor and mentor during this research. Furthermore, I would like to express my greatest gratitude to my family and my fiance for their patience and love over so many years.

APRIL 2011 Okan DOĞRU

TABLE OF CONTENTS

Page

ABBREVIATIONS

LBM	:	Lattice Boltzmann Method
DEM	:	Discrete Element Method
CFD	:	Computational Fluid Dynamics
BGK	:	Bhatnagar-Gross-Krook
DFR	:	Discrete Functional Representation
RBC	:	Red Blood Cell
WBC	:	White Blood Cell
TF	:	Tissue Factor
vWF	:	von Willebrand Factor

LIST OF FIGURES

Page

COMPUTATIONAL BLOOD CLOTTING MODELLING WITH COUPLED LATTICE BOLTZMANN AND DISCRETE ELEMENT METHODS

SUMMARY

One of the most important and complex physiologic system is the clotting mechanism. Blood must flow freely through the blood vessels so as to sustain life. But if a blood vessel is traumatized, the blood flow must be controlled by a mechanism to prevent flow outside from the blood vessels. Thus, to stop the flow of blood, the blood must provide a system that can be activated instantaneously and contained locally. This system is called the clotting mechanism.

The clotting mechanism requires two interacting processes known as blood platelet aggregation and coagulation. The aggregation of blood platelets is normally induced by the connection of chemicals with the blood plasma from the damaged endothelium in a traumatized blood vessel. When bleeding occurs, some of the chemical reactions change the surface of the platelets to make them sticky. Sticky platelets are said to have become activated. These activated platelets begin to aggregate at the wall of the blood vessel around the site of bleeding, and in a shorter time they form a white clot around there. The traumatized blood vessel also triggers a series of enzymatic reactions, leading to the process of blood coagulation. The activated coagulation proteins engage in a cascade of chemical reactions that finally produce a substance called fibrin. Fibrin can be thinkable as a long, sticky string. Fibrin strands stick to the exposed endothelium, clumping together and forming a web like complex of strands. Red blood cells become caught up in the web, and a red clot forms. The strands of fibrin bind the blood cells together, and tightened the clot to make it stable. A mature blood clot consists of platelets, red blood cells and fibrin strands.

At the present study, we considered a coupled Lattice Boltzmann Method (LBM) and Discrete Element Method (DEM) for the numerical modelling of the blood clot formation. We considered LBM for blood plasma flow simulation and DEM for thrombi formation due to cell aggregation/coagulation modelling.

LATTICE BOLTZMANN VE DISCRETE ELEMENT YÖNTEMLERİ KULLANILARAK KANIN PIHTILAŞMASININ MODELLENMESİ

ÖZET

Önemli ve karmaşık olan fizyolojik sistemlerden biride pıhtılaşma mekanizmasıdır. Hayatımızı sürdürebilmemiz için kan damarlarımızda serbestçe akmalıdır. Peki ya damarımızdan biri zedelenirse, kanın damarlarımız dışına akmasının engellenmesi için bir mekanizma tarafından kontrol altına alınması gerekmektedir. Kanın akışını durdurmak için kan ani ve yerel olarak oluşan bir sistem meydana getirmelidir. Bu sisteme pıhtılaşma mekanizması denilmektedir.

Pıhtılaşma mekanizması trombosit birikmesi ve koagülasyon olarak bilinen iki etkileşimli sürece ihtiyaç duymaktadır. Zarar görmüş bir damar içerisindeki kanın zedelenen endotelyumdaki kimyasallarla temas etmesiyle trombositlerin birikmesi süreci tetiklenmektedir. Kanama meydana geldiğinde, bazı kimyasal tepkimeler trombositlerin yüzeylerinin yapışkan özelliği kazanmasına sebep olmaktadırlar. Yapışkan olan trombositlere aktive olmuşta denilebilir. Aktive olmuş trombositler kanamanın meydana geldiği alanın çevresinde birikmeye başlarlar ve kısa bir süre içerisinde beyaz pıhtı denilen yapıyı oluştururlar. Ayrıca koagülasyon sürecinin başlaması için zarar gören damar bir takım enzimatik tepkimeleri tetikler. Aktive olan koagülasyon proteinleri fibrin denilen son ürünü elde edebilmek amacıyla kademeli bir kimyasal tepkimeler zincirine girerler. Fibrinler uzun yapışkan şeritler olarak düşünülebilirler. Fibrin şeritleri zarar gören endotel dokuya yapışırlar ve ağ şeklinde karmaşık bir yapı oluştururlar. Alyuvarlar bu karmaşık ağ yapısına takılırlar ve böylece kırmızı pıhtı oluşur. Fibrin şeritleri kan hücrelerinin birbirlerine sıkıca bağlanmasını sağlarlar ve daha stabil bir pıhtı için onları iyice sıkıştırırlar. Olgunlaşan bir pıhtı, içerisinde trombosit, alyuvar ve fibrin şeritlerini barındırır.

Bu çalışmada, kanın pıhtılaşmasının sayısal olarak modellenmesi için birleştirilmiş Lattice Boltzmann (LBM) ve Discrete Element (DEM) yöntemlerinin kullanılması düşünülmüştür. Kan plazmasının akışı için LBM ve hücrelerin birikimiyle trombüs oluşumu için DEM yöntemleri uygun görülmüştür.

1. INTRODUCTION

Blood is a specialized bodily fluid that delivers necessary substances, such as nutrients and oxygen, to the cells and transports waste products away from those same cells.

The 8% of human body weight consists of blood. Its average density is approximately 1060 kg/m^3, very close to pure water's density of 1000 kg/m^3. The average adult has a blood volume of approximately 5 liters. It is composed with plasma and several kinds of cells; these formed elements of the blood are red blood cells (RBCs, erythrocytes), white blood cells (leukocytes), and platelets (thrombocytes). If we think about the total volume of the blood, the plasma constitutes about 54.3%, the red blood cells about 44% and white cells about 0.7% of whole blood.

Whole blood (cells and plasma) shows non-Newtonian, viscoelastic fluid dynamics; its flow properties are adapted to flow effectively through tiny capillary blood vessels with less resistance than plasma by itself. In addition, if all human hemoglobin were free in the plasma rather than being contained in RBCs, the circulatory fluid would be too viscous for the cardiovascular system to function effectively.

As the existence of such a fluid being critical for life, blood must flow freely in our vessels. But if a vessel is traumatized, the blood flow must be controlled by a mechanism to prevent flow outside from the vessels. The clotting mechanism, which is named as blood coagulation, is the system of controlling the flow of blood after the vascular injuries. The phenomenon of coagulation is of enormous physiological importance. Its purpose is to stop further hemorrhage. When bleeding occurs, the shed blood coagulates and the bleeding vessels become plugged off by the clot. The retraction of the clot compresses the ruptured vessels further and in this way bleeding is stopped. Also It must be in a well regulated balance. Thus, the disorders of coagulation can lead to vital complications such as an increased risk of bleeding (hemorrhage) or obstructive clotting (thrombosis).

The current work presents a coupled Lattice Boltzmann (LBM) and Discrete Element Method (DEM) approach for the numerical modelling of the blood clotting mechanism.

The blood plasma flows are being modelled by the Lattice Boltzmann Method (LBM), while cell aggregation/coagulation being modelled by the Discrete Element Method.

In addition to classical Finite Volume and Finite Element based Computational Fluid Dynamics (CFD) solvers, the Lattice Boltzmann Method has emerged as a powerful numerical technique for solving fluid dynamics. This method is suitable for the simulation of fluid flow within time-varying and complicated computational boundary geometries.

Discrete Element Method is one of the powerful numerical modeling method to model the kinematic and dynamic behaviours of discontinuous bodies (like blood cells). These bodies can interact with each other. Nowadays, Discrete Element Method can simulate millions of particles on a single processor with progress of nearest neighbour sorting algorithms.

Tightly coupled interactions of blood flow and Red Blood Cells (RBC) are modelled by both LBM and DEM methods. Interactions are considered as particle (RBC) - particle (RBC) and particle (RBC) - blood flow and simulated by coupled LBM and DEM technique.

2. LITERATURE REVIEW

Nowadays, because of the abnormalities of coagulation system, people are having exceedingly important ailments. Therefore, the blood coagulation simulations are considered as being challenging topics currently. Especially, in the years after the millennium by using the accelerated computation power, blood coagulation simulations began to take place with different techniques in the literature.

In the literature, some of the studies are dealing with the blood coagulation system as a biochemical system. In these studies, the researchers are only focusing on to the concentrations of zymogens and chemical reactions about the blood coagulation system. As it can be seen from the studies [2–4] that, the mechanical effects of cardiovascular system were ignored and only chemical reactions and concentrations of coagulation factors were simulated in order to understand the blood coagulation system and its abnormalities. In these simulations, they took the whole coagulation system as an enzymatic activity. With this idea, they create some set of dynamic equations to present the whole coagulation system. Each of dynamic equations represents a mass balance of one of the chemicals involved [2]. Though these simulations, they can research effects of coagulation factors deficiencies but they did not mention any of the mechanical effects of blood flow or structures of vessels. So it can be concluded that, the whole blood coagulation can not be simulated only as a biochemical system.

On the other hand, some researchers simulating the blood coagulation system as a single blood flow problem. For these type of studies [5, 6], the coagulation system triggered from mechanical conditions and growing mechanism is fed by the mechanical conditions of the blood flow. In these studies, they assumed that the blood was only consisted of plasma. In the Bernsdorf's study, to simulate the clotting process numerically, they extended the Lattice Boltzmann Method in two ways: (1) an advection diffusion scheme for a passive scalar was applied in order to estimate the residence time of the fluid (blood), and (2) a solidification procedure depending on the age of the fluid [5]. In our view, blood coagulation system can not be simulated as a single fluid flow condition problem without the interactions of the blood cells.

Due to the disadvantages of separated biochemical and biomechanical blood coagulation simulations, we research literature for tightly coupled models. In the literature, there are less number of studies on the simulation of blood coagulation in both biochemical and biomechanical perspective. So, the main objective of our study is to couple the biochemical effects with biomechanical conditions for the simulation of the blood coagulation system but in this study we only created a base system for aggregation of blood cells.

To achieve our goal, firstly we must develop a generic simulation for the flow of blood plasma and blood cells together. In this study, the center of the research is the simulation of blood coagulation through the perspective of plasma flow including the blood cells. For the flow simulation of the blood plasma we used Lattice Boltzmann Method where as for the collisions of the blood cells inside the plasma, Discrete Element Method was used.

Lattice Boltzmann Method is a new alternative approach to classical Computational Fluid Dynamics simulations. Due to its particulate nature, it has some advantages on the parallelization of an algorithm. So, in the near future, the interest on this method is going to be fairly increased. There are many studies about Lattice Boltzmann method but especially Sukop's [7] and Wagner's [8] books are better references for the basics of this technique. Also, for the simulations of complex flow with LBM, Bernsdorf's thesis [9] can be a good reference.

On the other hand, Discrete Element Method is becoming widely accepted as an effective method of addressing engineering problems in granular and discontinuous materials. It was pioneered and developed by P.A. Cundall [10]. Nowadays, many researchers are using and developing this technique. In addition to Cundall's studies, we have benefited from the Zienkiewicz's [11] and Munjiza's [12] books. In the Munjiza's book, the main subject is about the combined finite-discrete element method. The combined finite-discrete element method is focusing on the problems which are involving transient dynamics of systems comprising a large number of deformable bodies that interact with each other [12]. Despite this, for now we used rigid discrete particles that interact with each other.

In order to coupling these two powerful method (LBM and DEM), the literature was searched deeply. There are very limited numbers of studies about coupling the LBM

with DEM. In the literature, the most important reference is the Feng's study [13]. This study presents essential numerical procedures in the context of the coupled Lattice Boltzmann Method (LBM) and Discrete Element Method (DEM) solution strategy for the simulation of particle transport in turbulent fluid flows. In Feng's study, the key computational issues involved are (1) the standard LBM formulation for the solution of incompressible fluid flows, (2) the incorporation of large eddy simulation (LES)-based turbulence models in the LBM equations for turbulent flows, (3) the computation of hydrodynamic interaction forces of the fluid and moving particles; and (4) the DEM modelling of the interaction between solid particles.

In our study, we created a simulation platform about particle transport in fluid flows through the enlightenment by Feng's study [13]. As we discussed above, the main objective of our study is simulating the both biochemical and biomechanical effects over the blood coagulation system. So we modelled the tightly coupled interactions of blood flow and blood cells. In an arterial flow for the aggregation of the blood cells, we created a clotting force which can take both zymases' and flow effects together. When the blood cells entered the area of the aggregation, they were influenced by a central force. The blood cells, which the effect of fluid flow force is lower than the clotting force, were aggregated at the clotting area. As a result, we constructed a simulation platform, which can take both influences of the biochemical and biomechanical conditions over the blood coagulation system by the help of clotting force.

3. BLOOD COAGULATION

3.1 Coagulation Process

Blood coagulation is a very complex process of the cardiovascular system. It is the important part of haemostasis (the preventing process of bleeding from a damaged vessel), wherein a damaged blood vessel wall is covered by the blood cells and fibrin containing clot to stop bleeding and begin repair of the damaged vessel. Also disorders of blood coagulation can cause to an increased risk of bleeding (hemorrhage) or obstructive clotting (thrombosis).

Blood coagulation begins almost instantly after an injury of the blood vessel's endothelium (lining of the vessel). When the tissue factor (TF) contact with the blood through the injury, it initiates changes of blood platelets and the fibrinogen protein, which is a clotting factor. Triggered platelets immediately form a plug at the injury area; this is called primary haemostasis. Then secondary haemostasis occurs simultaneously: The coagulation factors or clotting factors, respond in a complex cascade to form fibrin strands from fibrinogen, which strengthen the platelet plug with catching the other blood cells especially the red blood cells (see Figure 3.1).

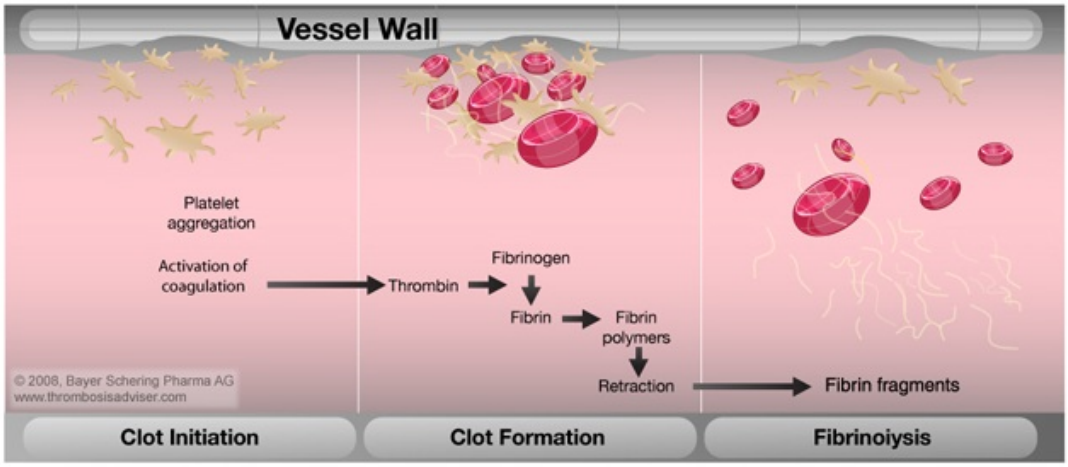

Figure 3.1: The Coagulation Schematic.

3.1.1 Platelet activation

For the activation of fibrinogens, firstly platelets must be activated. With the damage of blood vessel's wall, subendothelium proteins exposes. Under the endothelium, the most known protein is von Willebrand factor (vWF). Von Willebrand factor is a protein, which is secreted by healthy endothelium. It is main duty is forming a layer between the endothelium and underlying basement membrane. With the damage of endothelium, the normally isolated, underlying vWF activates Factor VIII, collagen, and other clotting factors. With the vWF's triger, platelets bind to collagen with surface collagen specific glycoprotein Ia/IIa receptors. This adhesion is strengthened with the help of von Willebrand factor, which forms additional links between the collagen fibrils and the platelets glycoprotein Ib/IX/V. Through these adhesions, the platelets become active.

After the activation of platelets, the contents of stored granules release into the blood plasma. The granules include ADP, platelet-activating factor (PAF), platelet factor 4, thromboxane A2 (TXA2), serotonin and vWF, which, in turn, activate additional platelets. Because of the increased calcium concentration in the platelets' cytosol, Gq-linked protein receptor cascade is become active. Also the calcium activates protein kinase C, which, in turn, activates PLA2 (phospholipase A2). Then PLA2 modifies the integrin membrane glycoprotein IIb/IIIa, increasing its affinity to bind fibrinogen. Activated platelets' shapes change from spherical to stellate. And the glycoprotein IIb/IIIa cross links with the fibrinogen for aggregation of adjacent platelets.

3.1.2 Coagulation cascade

The coagulation cascade has two pathways which lead to fibrin formation. These pathways are extrinsic pathway (tissue factor pathway), and intrinsic pathway (contact activation pathway). At the end of the process these two pathways joined to a common pathway. The pathways are a series of reactions, in which a zymogen of a serine protease and its glycoprotein cofactor are activated to become active components that then catalyze the next reaction in the cascade. As a result of these series of reactions cross-linked fibrins are processed (see Figure 3.2). In generally the coagulation factors are indicated by Roman numerals. In order to specify the activated forms of factors, a lowercase "a" appended at the end of Roman numerals.

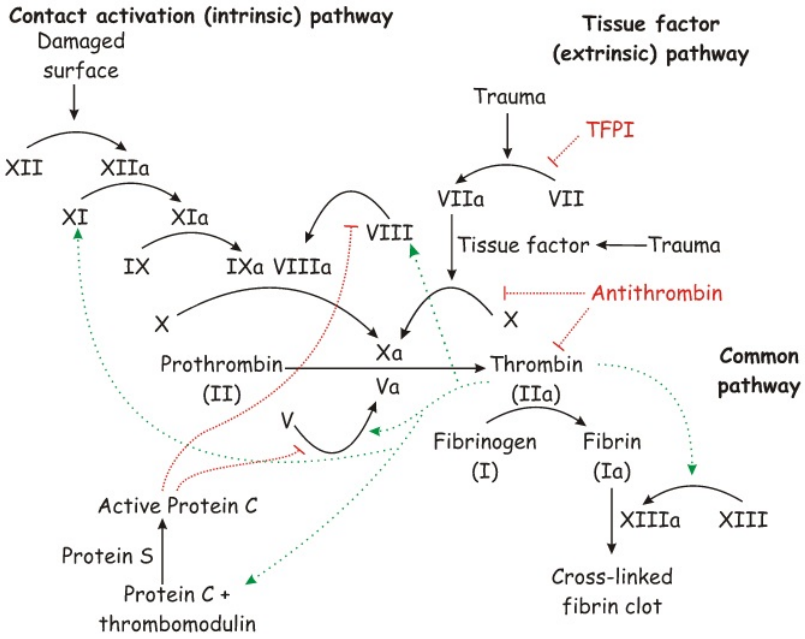

Figure 3.2: The Coagulation Cascade.

In generally, coagulation factors are serine proteases, but there are some exceptions. As an example, Factor XIII is a transglutaminase and FVIII and FV are glycoproteins. And in the circulation the coagulation factors stand as inactive zymogens. The coagulation cascade is classically divided into three pathways. The extrinsic and intrinsic pathways both activate the "final common pathway" of factor X, thrombin and fibrin.

3.1.2.1 Extrinsic pathway (Tissue factor pathway)

The main role of the extrinsic pathway (Tissue factor pathway) is generating a thrombin burst, a process by which thrombin is released instantaneously. The thrombin is the most important enzyme of the coagulation in terms of its feedback activation roles. On the other hand, the FVIIa factor is higher amount of than any other activated coagulation factor in the circulation.

- Following damage to the blood vessel, FVII leaves the circulation and comes into contact with tissue factor (TF) expressed on tissue-factor-bearing cells (stromal fibroblasts and leukocytes), forming an activated complex (TF-FVIIa).
- TF-FVIIa activates FIX and FX.
- FVII is itself activated by thrombin, FXIa, FXII and FXa.

- The activation of FXa by TF-FVIIa is almost immediately inhibited by tissue factor pathway inhibitor (TFPI).
- FXa and its co-factor FVa form the prothrombinase complex, which activates prothrombin to thrombin.
- Thrombin then activates other components of the coagulation cascade, including FV and FVIII (which activates FXI, which, in turn, activates FIX), and activates and releases FVIII from being bound to vWF.
- FVIIIa is the co-factor of FIXa, and together they form the "tenase" complex, which activates FX; and so the cycle continues.

3.1.2.2 Intrinsic pathway (Contact activation pathway)

The intrinsic pathway starts with the formation of primary complex on collagen by high-molecular-weight kininogen (HMWK), prekallikrein, and FXII. Prekallikrein is converted to kallikrein and FXII activated to FXIIa. FXIIa converts FXI into FXIa. Factor XIa activates FIX, which with FVIIIa form the tenase complex, which activates FX to FXa. The intrinsic pathway has in initiating clot formation can be illustrated by the fact who has deficiencies of HMWK, FXII and prekallikrein do not have a bleeding disorder.

3.1.2.3 Final common pathway

The thrombin's primary role is the activation of fibrinogen to fibrin, which is building block of a hemostatic plug. Besides, it activates Factor XIII, which forms covalent bonds that crosslink the fibrin polymers that form from activated monomers and their inhibitor protein C, and also it activates Factors VIII and V. Following activation by the intrinsic or extrinsic pathways, for forming the tenase complex by the continued activation of FVIII and FIX, the coagulation cascade is maintained in a prothrombotic state until it is down regulated by the anticoagulant pathways.

3.2 Blood Clot

At the coagulation cascades some chain reactions occurs and platelets and fibrinogens activated. The active platelets become a sticky structure. At the site of injury, platelets change their shapes from round to spiny and release proteins and other substances that

help catch more platelets and clotting proteins. By the help of fibrin strands they catch other blood cells, especially red blood cells. Also with the red blood cells, the blood clot's color changes to red. In a fully developed blood clot, it has mostly red blood cells in its structure.

The series of reactions that cause platelets and proteins to create blood clots are balanced by other reactions that stop the clotting process and dissolve clots after the blood vessel has repaired. If this control system fails, blood vessel injuries can trigger clotting throughout the body. The tendency to clot too much is called hypercoagulation. This blood clots inside the blood vessels can cause to vital complications.

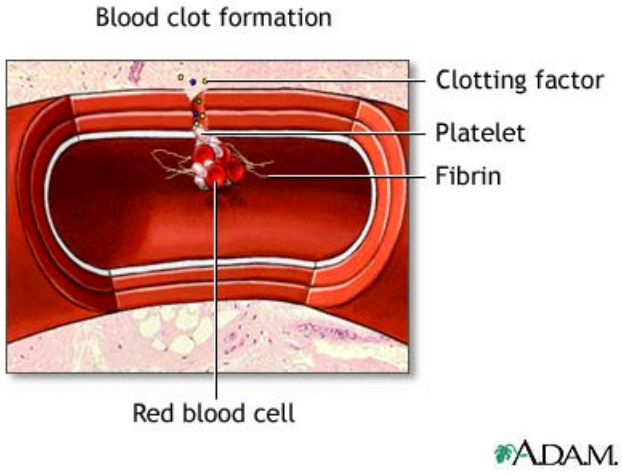

Figure 3.3: Blood Clot Formation.

3.3 Clotting Disorders

Clotting disorders is a term used to describe a group of conditions often repeated and over an extended period of time, for excessive clotting. There is an increased tendency on the clotting disorders. These disorders include inherited conditions such as protein C deficiency, protein S deficiency, Factor V Leiden, anti-thrombin deficiency and prothrombin 20210A mutations.

Thrombophilia affects too many people around the world. The most common inherited abnormality in this class is Factor V Leiden. It affects approximately 5% to 7% of the Caucasian population of European descent in the United States [14].

People who experience episodes of thrombosis, either as a repeated event or as an isolated event, may be affected with a thrombophilic disorder. There are people who

have inherited the gene, who have an increased tendency for thrombosis, but may never personally experience a blood clot. Many people can have a thrombophilic condition and never experience a thrombosis.

3.3.1 Thrombosis

Thrombosis is a medical term which is the formation of a blood clot inside the blood vessel. The clot inside the blood vessel named as thrombus and with this blood clot blood vessel can be plugged (see Figure 3.4). Thrombus can form in both arteries and veins of the cardiovascular system. If the formation of a thrombus within a vein, it is named as venous thrombosis. If the formation of a thrombus within an artery, it is named as arterial thrombosis. Venous thrombosis has several types like deep vein thrombosis, portal vein thrombosis, renal vein thrombosis etc.

Thrombus formation, which is caused by coagulation of the blood, can be occurred anywhere inside the cardiovascular system. If thrombus detaches itself and begins to travel through the body, which is named as embolus, it can plug very important vessels. When the thrombus occurs in one of the two main arteries of the heart, this condition can induce to heart attack.

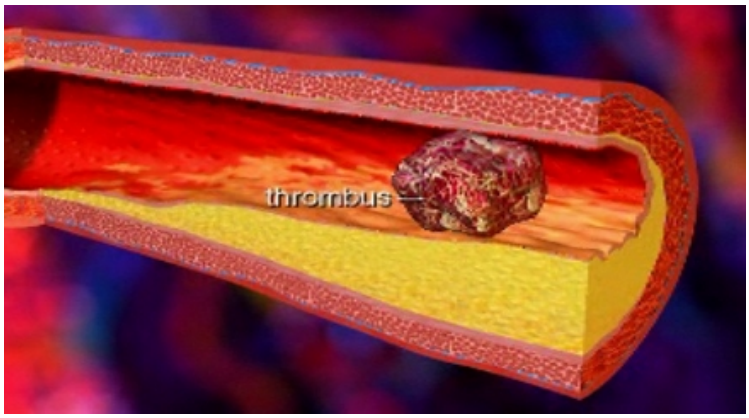

Figure 3.4: Thrombosis.

There are several causes of thrombosis. The most known are Virchows triad. These are endothelial injury, hemodynamic changes and hypercoagulability. The inner layer of the blood vessel (endothelium) can be damaged because of the high shear stress or hypertension. Moreover hemodynamic changes like stasis, varicose, mitral stenosis, and turbulence veins can cause thrombosis. Furthermore the hypercoagulability is the most important reason for the thrombosis disease. Hypercoagulability is a genetic

disorder about abnormality in the system of coagulation. This genetic disorder the patient's clotting factors can cause the formation of thrombus inside the blood vessel unnecessarily. Besides all of these, lifestyle habits such as smoking, alcohol, and obesity can serve as contributing reasons.

4. BLOOD FLOW AND BLOOD CELLS

4.1 Blood Flow

Blood is a specialised fluid which transports nutrients, oxygen and waste products through the network of vessels. Basically it is consists of plasma and blood cells. In large vessels (diameter greater than 1 mm) blood behaves can be accepted as a Newtonian fluid. However in smaller vessels, like capillaries, the blood behaviour is non-Newtonian. In the Türkeri's study, the differences of Newtonian and non-Newtonian fluid affects on the blood plasma simulations can be found [15]. However, in this study, we modelled the blood plasma as a Newtonian fluid.

Through the cardiovascular system, the blood flow is driven by the pumping of the heart. So, the pressure inside the arteries can be different from the veins. In our study, simulations was done with the consideration of an artery.

The red blood cells (RBC) have a very high amount in the blood. They are approximately 45% of blood by volume. Because of their semisolid structure and amount, they increase the viscosity of blood and change the behavior of the fluid.

The blood plasma, which is the only fluid part of the blood, makes up about 54.3% of the total blood volume. Also its density is between 1000 kg/m^3 and 1100 kg/m^3 depends only on temperature. The Reynolds number is typically on the order of 100 to 1000 for a medium-sized artery.

In our simulations, we used Poiseuille flow for modeling blood flow (see Figure 4.1). The velocity is initialized to zero, and converges only slowly to the expected parabola [16].

With the consideration of all above, we modeled blood flow with Lattice Boltzmann Method. In this study we used 2D LBM techniques. The computational domain is spatially discretized by the lattices, and an extremely regular model is used for the motion of the particles in Lattice Boltzmann Method. The nodes of the lattice confine the positions of particles. In our 2D model momentum change modelled with continuum

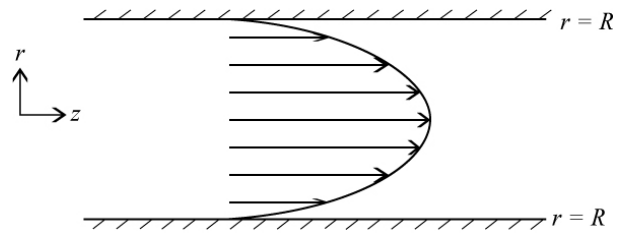

Figure 4.1: Poiseuille flow in a circular tube.

of velocity directions and magnitudes and with changing particle mass. These variables are described as 8 directions, 3 magnitudes and 1 particle mass. Figure 4.2 shows the cartesian lattice and the velocities. The e_i where $i = 0, 1, ..., 8$ is a direction index and $e_0 = 0$ represents particles at rest. This type of model is D2Q9 model (see Figure 4.2). It is a 2 dimensional and 9 directional model. This discretization scheme was presented by Qian et al. [17] and now it is in common use. Velocities and momentums are effectively equivalent because of the uniform particle mass. (see Sukop et al. [7])

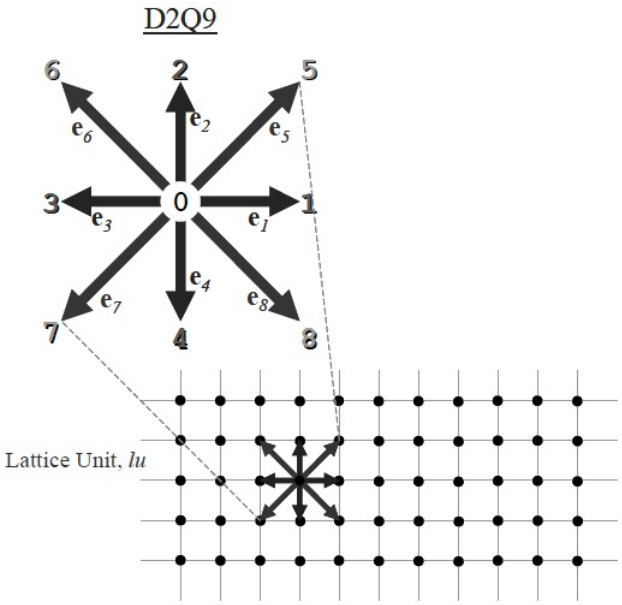

Figure 4.2: D2Q9 lattice and velocities.

The most common velocity indexing scheme is 1 lattice unit per time step ($1luts^{-1}$) for e_1 through e_4 and $\sqrt{2}luts^{-1}$ for e_5 through e_8. If their x and y components either 0 or $\pm$ 1, these velocities are exceptionally suitable. For streaming and collision of the particles via the distribution function, we used the BGK (Bhatnagar-Gross-Krook) approximation in our simulations.

4.2 Blood Cells

Basically blood is consist of plasma and blood cells that float in it. Also blood contains clotting factors, proteins and waste products. In vertebrates, blood is suspended in a liquid called plasma. The amount of plasma is 54.3% of whole blood. In the blood plasma it contains proteins, mineral ions, hormones, glucose, carbon dioxide and blood cells. The blood cells are mainly red blood cells (RBC)and white blood cells, including leukocytes and platelets. In vertebrates, the most abundant cell is RBC. Red blood cell's main duty is the transportation of oxygen to the cells with hemoglobin. In contrast, carbon dioxide is almost entirely transported extracellularly dissolved in plasma as bicarbonate ion.

All of the body tissues are dependent upon oxygen from red blood cells. Because of this dependency if the blood flow is cut off, the body tissues dies. So the transformation of oxygen must be never stopped. In the red blood cells of all vertebrates, hemoglobin is the iron containing oxygen transport metalloprotein. Also hemoglobin makes up 97% of the dry weight of red blood cells, and 35% of the total weight, including water. Because of this feature of RBC, they have a semisolid structure.

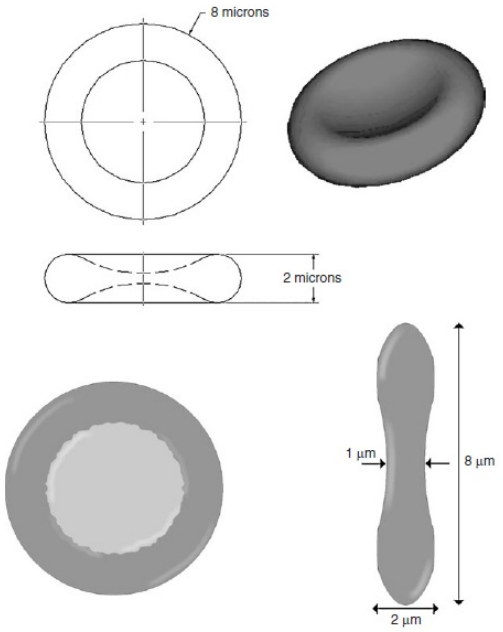

Figure 4.3: Shape of Red Blood Cells.

Typical human RBC has a disk diameter of $6-8\ \mu m$ and a thickness of $2\ \mu m$ (see Figure 4.3). These cells have a volume of about $90\ fL$ with a surface of about $136\ \mu m^2$, and can swell up to a sphere shape containing $150\ fL$, without membrane distension. Approximately an adult woman have about 4 to 5 million RBCs per microliter (cubic millimeter) of blood and an adult man about 5 to 6 million; people living at high altitudes with low oxygen tension will have more.

Due to the RBCs are the most common cells in the blood, mostly we used RBCs for aggregation in our blood coagulation simulations.

Also as a type of blood cell, white blood cells (WBC) are important of the body defence system against to foreign substance. The number of white blood cells is related to foreign substance but normally they are between $4\ x\ 10^9$ and $1.1\ x\ 10^{10}$ in a liter of blood. For a healthy adult WBCs are approximately 0.7% of whole blood.

Another important blood cell is the platelet. They are irregularly-shaped and colorless bodies. Because of their sticky surface for the coagulation system platelets have a very important mission. When bleeding from a wound suddenly occurs, the platelets gather at the injured area and attempt to block the blood flow immediately.

If the amount of platelets is too low, irrepressible bleeding can occur. However, if the amount of platelets is too high, blood clots can be formed inside the blood vessel (thrombosis), which may obstruct blood vessels and result in such events as a stroke, pulmonary embolism, myocardial infarction or the blockage of blood vessels to other parts of the body, such as arms or legs.

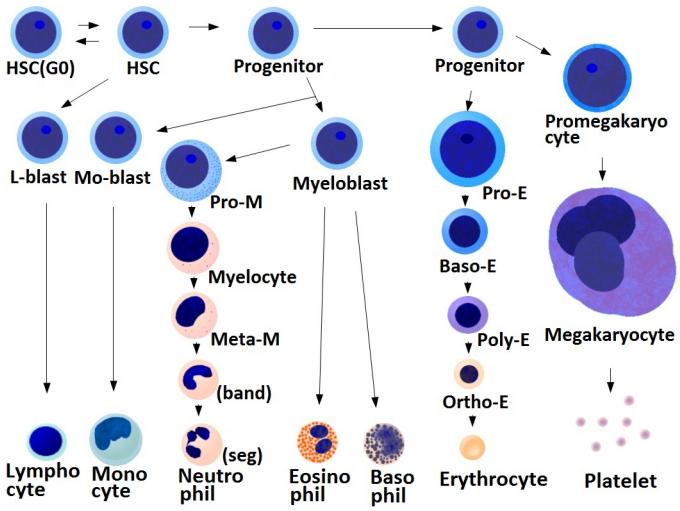

Figure 4.4: Blood Cells Differentiation Chart.

In our coagulation simulations, we modelled blood cells with discrete element method. In Discrete Element Method, the forces acting on the discontinuous bodies (particles like blood cells) are summed and the equations of motion of Newton and Euler are integrated to obtain the velocity and the position of the particles in the next time step.

In this study, the simulations were created with red blood cells. Also in coagulation process, because of their percentages in the whole blood, the clot substance consist of red blood cells (see Figure 4.5).

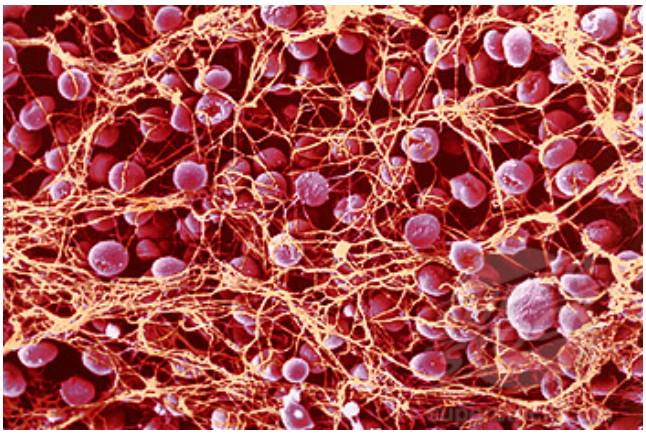

Figure 4.5: Red blood cells in a web of fibrin.

5. THE SIMULATION OF THROMBUS FORMATION

Thrombosis is a medical term which is the formation of a blood clot inside the blood vessel. With this clot the blood vessel can be plugged and caused to vital complications. Because of the vital importance of this disease, thrombosis must be understood perfectly. So in this study, we get this diseases as a basis of our blood coagulation simulations.

The thrombus formation simulation presents a coupled Lattice Boltzmann and Discrete Element approach for the numerical modeling of the thrombus formation. For the flow simulation of the blood plasma we used Lattice Boltzmann Method where as for the collisions and aggregation of the blood cells inside the plasma, Discrete Element Method was used.

Simulation based on Newtonian blood plasma flow and the flow was assumed as 2D Poiseuille flow. Our simulation domain was 400lu x 100lu (lu is the lattice unit and can be accepted as millimeter in this simulation), the fluid density was $1060kg/m^3$, Reynolds number was 1000 and for Lattice Boltzmann Method the time step was $\Delta t = 0.0001sec$. At the end of the domain we have a fattycore area, which the aggregation will start there (see Fig. 5.1).

Red Blood Cells were simulated with discrete element method using viscoelastic material model for the collisions of RBCs. Also the RBCs were modeled to resist shear flow and strain linearly with time when a stress is applied with viscoelasticity.

At this simulation, the discrete element method's time step was $\Delta t = 4.76e-6sec$, and RBCs' normal restitution coefficient $en = 0.3$ and tangential restitution coefficient $es = 0.3$. These parameters were used for calculating viscoelastic material's elastic and viscous coefficients. The friction angle was taken as $35rad$. For simplicity, we used circle particles for modeling the RBCs. The particles' mass were taken as $1e-17kg$.

For aggregation we used central force field technique. This force was supplanted for clotting factors' effects and called as clotting force. When the particles enter the area of aggregation, they were influenced by a central force. The particles which the fluid flow

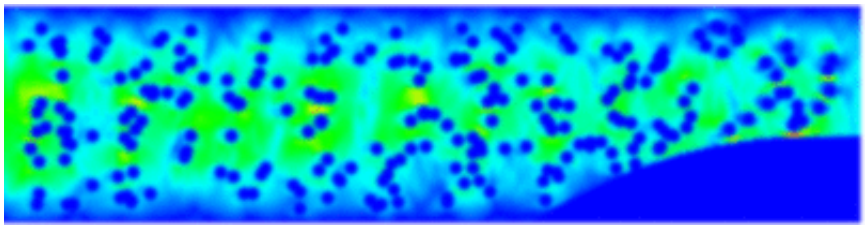

Figure 5.1: Starting position of the thrombus formation simulation.

force is lower than clotting force, were aggregate at the clotting area. Thus a thrombus can be occurred at the diseased area. For now, the clotting force is an imaginary force to trigger the cell aggregation mechanism so the clotting force does not depend on concentrations of thrombin. In the near future with a point of biochemical view, it is going to be bonded with the concentration of the thrombin and the production rate of the thrombin. In this simulation, we planned to create a biomechanical base system for the blood coagulation simulations without any biochemical effects.

6. NUMERICAL METHODS

In order to simulate the blood coagulation system, we used two numerical methods together. The blood plasma flows being simulated by the Lattice Boltzmann Method (LBM) [18], while thrombus formation due to cell aggregation/coagulation being modeled by the Discrete Element Method (DEM) [19].

6.1 Lattice Boltzmann Method (LBM)

Navier-Stokes and continuity are principles of the traditional fluid dynamics. It is given by,

$$\partial_t \rho + \nabla(\rho u) = 0 \tag{6.1}$$

and expresses that the density ρ is a locally conserved quantity and can only be changed if it is advected away by a flow with velocity u. So the change of the density ρ is given by the divergence of the current ρu. The main idea in the physical content of this equation is the density in this system which is locally conserved. For the local velocity u we need to couple Navier-Stokes equation with this equation,

$$\partial_t(\rho u) + \nabla(\rho uu) = -\nabla p + \nabla\sigma \tag{6.2}$$

where p is the local pressure and σ is a viscous stress tensor. For the stress we can write this equation,

$$\sigma = \eta\left[\nabla u + (\nabla u)^T\right] + \nu\nabla.u1. \tag{6.3}$$

To numerically integrate these equations we need to discretize the derivatives requiring first and second order derivatives. There are many possible discretizations of

these equations. Lots of these possible discretizations will only conserve mass and momentum up to the order of discretization. An alternative approach to these computational fluid dynamics simulations was invented in the late 1980s with the lattice gas methods. These methods allowed particles to move on a discrete lattice and local collisions conserved mass and momentum. This is the Lattice Boltzmann Method which has been extraordinarily successful for many applications including turbulence, multi-component and multi-phase flows as well as additional applications, including simulations of the Schrödinger equation.

6.1.1 The Boltzmann equation

The dynamics of the Boltzmann equation always mimimizes the H-Functional,

$$H(t) = \int dxdvf(x,v,t)log(f(x,v,t)) \tag{6.4}$$

This H-functional will be minimized by the equilibrium distribution function f^0 in a volume V for a given density n, mean momentum nu and energy $n\varepsilon = 1/2nu^2 + 3/2n\theta$. To minimize this H-functional we can use Lagrangian multipliers. With Lagrangian multipliers the H-functional adopts the following form:

$$\begin{aligned} H(t) = &\int dxdvf(x,v,t)log(f(x,v,t)) \\ &- \lambda_1 \left(nV - \int dxdvf(x,v,t) \right) \\ &- \lambda_{2\alpha} \left(nu_\alpha V - \int dxdvf(x,v,t)v_\alpha \right) \\ &- \lambda_3 \left(n\varepsilon V - \int dxdvf(x,v,t)\frac{v^2}{2} \right) \end{aligned} \tag{6.5}$$

With respect to the distribution function, we can calculate the functional derivative of the H-functional. Since the equilibrium distribution minimizes the H-functional this derivative has to vanish when the distribution is the equilibrium distribution $f = f^0$.

$$0 = \left. \frac{\delta H(t)}{\delta f} \right|_{f=f^0} = 1 + log(f^0) + \lambda_1 + \lambda_{2\alpha}v_\alpha + \lambda_3 \frac{v^2}{2} \tag{6.6}$$

Solving for the equilibrium distribution:

$$f^0 = exp\left[-1-\lambda_1+\frac{\lambda_2^2}{2\lambda_3}-\frac{\lambda_3}{2}\left(\frac{\lambda_2}{\lambda_3}+v\right)^2\right] \tag{6.7}$$

The new set of Lagrangian multipliers, a, b and c, can be written as,

$$f^0 = aexp\left[\frac{(b-v)^2}{c}\right] \tag{6.8}$$

As you can see that this expression does not depend on spatial variables. Thus, the solution will be homogeneous. By invoking the conservation laws, we can find the Lagrange multipliers

$$nV = \int dxdvf^0 nu_\alpha V = \int dxdvf^0 v_\alpha \frac{nu^2}{2}V + \frac{3}{2}n\theta V = \int dxdvf^0\frac{v^2}{2} \tag{6.9}$$

The equilibrium distribution can be found with solving these equations for a, b and c

$$f^0 = \frac{n}{(2\pi\theta)^{3/2}}exp\left[-\frac{(v-u)^2}{2\theta}\right] \tag{6.10}$$

which is known as the Maxwell-Boltzmann distribution.

6.1.2 Derivation of the hydrodynamic equations from the Boltzmann equation

The conservation equations for continuous fields are simply the macroscopic equations of motion. The general concepts involved the transport equations we derive not only applicable for dilute gases, which we require for the Boltzmann equation to apply, but also for much denser fluids. With this point of view a numerical method called "Lattice Boltzmann" has been developed for the simulation of fluid dynamics.

The Boltzmann equation is given by

$$\partial_t f + v\partial_x f + F\partial_v f = \int dv_1' dv_2' dv_2 (f_1' f_2' - f_1 f_2) P_{12\to 1'2'} \tag{6.11}$$

Solving this equation analytically is very challenging and can only be done for special cases.

6.1.2.1 The BGK approximation

The Bhatnagar, Gross and Krook noticed that the main effect of the collision term is to bring the velocity distribution function closer to the equilibrium distribution. The equilibrium distribution is given by

$$f^0(v) = \frac{n}{(2\pi\theta)^{3/2}} e^{-(v-u)^2/2\theta} \tag{6.12}$$

where n is the number density of particle, u is the mean velocity and $\theta = kT$ is the temperature. These macroscopic quantities can be given by moments of the distribution function:

$$\int f = n \tag{6.13}$$

$$\int f v_\alpha = n v_\alpha \tag{6.14}$$

$$\int f v^2 = n u^2 + 3n\theta \tag{6.15}$$

Single relaxation time approximation is the simplest way for approximating the collision term.

$$\int dv_1' dv_2' dv_2 (f_1' f_2' - f_1 f_2) P_{12\to 1'2'} \approx \frac{1}{\tau}(f^0 - f) \tag{6.16}$$

Because of this approximation's important feature the mass, momentum and energy can be still exactly conserved by the collision term. With this approximation the Boltzmann equation can be written as,

$$\partial_t f + v\partial_x f + F\partial_v f = \frac{1}{\tau}(f^0 - f) \tag{6.17}$$

This expression can be used for to approximate the probability density function by the equilibrium distribution and its derivatives.

$$f = f^0 - \tau(\partial_t f + v\partial_x f + F\partial_v f) \tag{6.18}$$

6.1.2.2 Moments of the equilibrium distribution function

The distribution function can be expressed in terms of the equilibrium distribution function. Thus, velocity moments of the equilibrium distribution function can be written as,

$$\int f^0 = n \tag{6.19}$$

$$\int f^0(v_\alpha - u_\alpha) = 0 \tag{6.20}$$

$$\int f^0(v_\alpha - u_\alpha)(v_\beta - u_\beta) = n\theta\delta_{\alpha\beta} \tag{6.21}$$

$$\int f^0(v_\alpha - u_\alpha)(v_\beta - u_\beta)(v_\gamma - u_\gamma) = 0 \tag{6.22}$$

$$\int f^0(v_\alpha - u_\alpha)(v_\beta - u_\beta)(v-u)^2 = 5n\theta^2\delta_{\alpha\beta} \tag{6.23}$$

These are derived using Gaussian integrals.

6.1.2.3 Mass conservation

The mass conservation equation can be found with integrating over the Boltzmann equation.

$$\begin{aligned}&\partial_t \int dv f + \partial_\alpha \int dv f v_\alpha + F\int dv \partial_v f = \frac{1}{\tau}\int dv(f^0 - f)\\ &\Leftrightarrow \partial_t n + \partial_\alpha(nu_\alpha) = 0\end{aligned} \tag{6.24}$$

which is the continuity equation.

6.1.2.4 Momentum conservation

For obtaining the momentum conservation equation the Boltzmann equation was multiplied with v_α and integrated.

$$\partial_t \int dv f v_\alpha + \partial_\beta \int dv f v_\alpha v_\beta + F_\beta \int dv \partial_{v_\beta} f v_\alpha = \frac{1}{\tau} \int dv (f^0 - f) v \tag{6.25}$$

$$\partial_t (n u_\alpha) + \partial_\beta \int dv f v_\alpha v_\beta - n F_\alpha = 0 \tag{6.26}$$

We now need to use equation (**6.18**) to approximate

$$\begin{aligned} \int dv f v_\alpha v_\beta = & \int dv f^0 v_\alpha v_\beta \\ & - \tau \left(\partial_t \int dv f^0 v_\alpha v_\beta + \partial_\gamma \int dv f^0 v_\alpha v_\beta u_\gamma + n F_\alpha u_\beta + n u_\alpha F_\beta \right) + O(\partial^2) \end{aligned} \tag{6.27}$$

To first order in derivatives conservation equation now reads

$$\partial_t (n u_\alpha) + \partial_\beta (n u_\alpha u_\beta) = -\partial_\alpha (n\theta) + n F_\alpha \tag{6.28}$$

The equation that appears above is known as the Euler equation. With using the continuity equation we can also write it as

$$\partial_t u_\alpha + u_\beta \partial_\beta u_\alpha = -\frac{1}{n} \partial_\alpha (n\theta) + F_\alpha \tag{6.29}$$

To calculate the equations of motion to second order in the derivatives we need to evaluate the higher order terms in equation (**6.27**) .

$$
\begin{aligned}
&\partial_t \left(\int f^0 v_\alpha v_\beta \right) \\
&\qquad = \partial_t (n u_\alpha u_\beta + n\theta \delta_{\alpha\beta}) \\
&\qquad = \partial_t (n u_\alpha) u_\beta + n u_\alpha \partial_t u_\beta + \partial_t n\theta \delta_{\alpha\beta} + n\partial_t \theta \delta_{\alpha\beta} \\
&\qquad = -\partial_\gamma (n u_\alpha u_\gamma) u_\beta - \partial_\alpha (n\theta) u_\beta - n F_\alpha u_\beta \\
&\qquad - n u_\alpha u_\gamma \partial_\gamma u_\beta - u_\alpha \partial_\beta (n\theta) - n u_\alpha F_\beta \\
&\qquad - \partial_\gamma (n u_\gamma) \theta \delta_{\alpha\beta} - n u_\gamma \partial_\gamma (\theta \delta_{\alpha\beta}) - \frac{2}{3} \partial_\gamma u_\gamma \theta \\
&\qquad = -\partial_\gamma (n u_\alpha u_\beta u_\gamma) - \partial_\beta (n\theta) u_\alpha - \partial_\alpha (n\theta) u_\beta - n(F_\alpha u_\beta + u_\alpha F_\beta) \\
&\qquad - \partial_\gamma (n\theta u_\gamma) \delta_{\alpha\beta} - \frac{2}{3} n\theta \partial_\gamma u_\gamma
\end{aligned} \tag{6.30}
$$

$$
\partial_\gamma \int f^0 v_\alpha v_\beta v_\gamma = \partial_\beta (n\theta u_\alpha) + \partial_\alpha (n\theta u_\beta) + \partial_\gamma (n\theta u_\gamma) \delta_{\alpha\beta} + \partial_\gamma (n u_\alpha u_\beta u_\gamma) \tag{6.31}
$$

$$
\partial_t \int dv f^0 v_\alpha v_\beta + \partial_\gamma \int dv f^0 v_\alpha v_\beta v_\gamma = n\theta (\partial_\alpha u_\beta + \partial_\beta u_\alpha) - \frac{2}{3} n\theta \partial_\gamma u_\gamma \tag{6.32}
$$

This expressions can be used to obtain the first order momentum conservation from equation

$$
n\partial_t u_\alpha + n u_\beta \partial_\beta u_\alpha = -\partial_\alpha (n\theta) + n F_\alpha + \partial_\beta \left[\eta \left(\partial_\beta u_\alpha + \partial_\alpha u_\beta - \frac{2}{3} \partial_\gamma u_\gamma \delta_{\alpha\beta} \right) \right] \tag{6.33}
$$

where $\eta = n\theta\tau$ is the viscosity. This equation is known as the Navier-Stokes Equation.

6.1.2.5 Energy conservation

For obtaining the energy equation the Boltzmann equation multiplied with $(v-u)^2$ and integrated

$$\int dv\partial_t f(v-u)^2 + \int dv\partial_\alpha f v_\alpha (v-u)^2 + F_\alpha \int dv\partial_{v_\alpha} f(v-u)^2 = \frac{1}{\tau}\int dv(f^0 - f)(v-u)^2$$

$$\Leftrightarrow \partial_t \int dv f(v-u)^2 + \int dv f 2(v_\alpha - u_\alpha)\partial_t u_\alpha$$

$$+ \partial_\alpha \int dv f v_\alpha (v-u)^2 + \int dv f v_\alpha 2(v_\beta - u_\beta)\partial_\alpha u_\beta = 0$$

$$\Leftrightarrow \partial_t \int dv f(v-u)^2 + \partial_\alpha \int dv f v_\alpha (v-u)^2 + 2n\theta\partial_\alpha u_\alpha$$

$$- \tau\left[\int \partial_t (v_\alpha - u_\alpha)(v_\beta - u_\beta)\int \partial_\gamma f^0 v_\gamma (v_\alpha - u_\alpha)(v_\beta - u_\beta)\right]\partial_\alpha u_\beta = 0$$

$$\Leftrightarrow 3\partial_t(n\theta) + \partial_\alpha \int dv f v_\alpha (v-u)^2 + 2n\theta\partial_\alpha u_\alpha$$

$$- \tau\partial_\alpha u_\beta\left(\partial_\alpha u_\beta + \partial_\beta u_\alpha - \frac{2}{3}\partial_\gamma u_\gamma \delta_{\alpha\beta}\right) = 0 \qquad \textbf{(6.34)}$$

The remaining integral is need to be approximated by using equation (**6.18**)

$$\int dv f v_\alpha (v-u)^2$$

$$= dv f^0 v_\alpha (v-u)^2 - \tau[\int dv\partial_t f v_\alpha (v-u)^2 + \int dv\partial_\beta f v_\alpha v_\beta (v-u)^2$$

$$+ \int dv\partial_v f v_\alpha (v-u)^2]$$

$$= 3n\theta u_\alpha - \tau[\int dv\partial_t f^0 v_\alpha (v-u)^2 + \int dv\partial_\beta f^0 v_\alpha v_\beta (v-u)^2$$

$$- 5n\theta F_\alpha] + O(\partial^2) \qquad \textbf{(6.35)}$$

For the zeroth order the energy conservation equation can be written as

$$\partial_t\theta + u_\alpha\partial_\alpha\theta = -\frac{2}{3}\partial_\alpha u_\alpha\theta + O(\partial^2) \qquad \textbf{(6.36)}$$

again the continuity equation (**6.24**) was used. To obtain the first order equation the two integrals in equation (**6.35**) must be evaluated.

$$\int dv \partial_t f^0 v_\alpha (v-u)^2$$

$$= \partial_t \int f^0 v_\alpha (v-u)^2 + \int f^0 v_\alpha 2(v_\gamma - u_\gamma)\partial_t u_\gamma$$
$$= \partial_t (3n\theta u_\alpha) + 2n\theta \partial_t u_\alpha$$
$$= 3\theta[-\partial_\beta (nu_\alpha u_\beta) - \partial_\alpha (n\theta) + nF_\alpha] + 3nu_\alpha(-u_\beta \partial_\beta \theta - \frac{2}{3}\partial_\beta u_\beta \theta)$$
$$+ 2n\theta[-u_\beta \partial_\beta u_\alpha - \frac{1}{n}\partial_\alpha (n\theta) + f_\alpha]$$
$$= \partial_\beta (-3\theta n u_\alpha u_\beta) - 2n\theta \partial_\beta (u_\alpha u_\beta) - 5\theta \partial_\alpha (n\theta) + 5nF_\alpha \quad \textbf{(6.37)}$$

For the second integral,

$$\int dv \partial_\beta f^0 v_\alpha v_\beta (v-u)^2$$

$$= \partial_\beta \int f^0 v_\alpha v_\beta (v-u)^2 + \int f^0 v_\alpha v_\beta 2(v_\gamma - u_\gamma)\partial_\beta u_\gamma$$
$$= \partial_\alpha \int dv f^0 (v_\alpha - u_\alpha)(v_\beta - u_\beta)(v-u)^2 - \partial_\beta (3n\theta u_\alpha u_\beta)$$
$$+ 2n\theta (u_\alpha \partial_\beta u_\beta + u_\beta \partial_\beta u_\alpha)$$
$$= \partial_\alpha (5n\theta^2) + \partial_\beta (3n\theta u_\alpha u_\beta) + 2n\theta \partial_\beta (u_\alpha u_\beta) \quad \textbf{(6.38)}$$

Both integrals from equation (**6.35**) and the forcing term can be combined,

$$\partial_\alpha (5n\theta^2) - 5\theta \partial_\alpha (n\theta) = 5n\theta \partial_\alpha \theta \quad \textbf{(6.39)}$$

Hence, the heat conduction equation can be found as,

$$\partial_t \theta + u_\alpha \partial_\alpha \theta = -\frac{2}{3}\partial_\alpha u_\alpha \theta + \frac{1}{n}\partial_\alpha (\frac{5n\theta}{3}\partial_\alpha \theta) + \tau \partial_\alpha u_\beta \left(\partial_\alpha u_\beta + \partial_\beta u_\alpha - \frac{2}{3}\partial_\gamma u_\gamma \delta_{\alpha\beta}\right) \quad \textbf{(6.40)}$$

6.1.3 Lattice Boltzmann

6.1.3.1 The Lattice Boltzmann equation

A simple discretization of the Boltzmann equation with BGK approximation (**6.17**) for the collision term can be written as

$$f(x+v_i,v_i,t+1)-f(x,v_i,t)+F(v_i)=\frac{1}{\tau}[f^0(n,u,\theta)-f(x,v_i,t)] \tag{6.41}$$

Here velocity space was discretized to a finite number of velocity vectors v_i, $x+v_i$ is new lattice position and t is the time which can only takes integer values. Because of the velocity vectors are fixed the equations can be writen as $f(x,v_i,t)\equiv f_i(x,t)$ and $F(v_i)\equiv F_i$. The force terms F_i are defined as a generalization of the force of equation (**6.17**), i.e. $F_i \leftrightarrow F_\alpha \partial_{v_\alpha} f$. Moments can be matched up like:

$$\sum_i F_i = \int dv F_\alpha \partial_{v_\alpha} f = 0 \tag{6.42}$$

$$\sum_i F_i v_{i\alpha} = \int dv F_\beta \partial_{v_\beta} f v_\alpha = -nF_\alpha \tag{6.43}$$

$$\sum_i F_i v_{i\alpha} v_{i\beta} = \int dv F_\gamma \partial_{v_\gamma} f v_\alpha v_\beta = -n(F_\alpha u_\beta + u_\alpha F_\beta) \tag{6.44}$$

$$\begin{aligned}\sum_i F_i v_{i\alpha} v_{i\beta} v_{i\gamma} = \int dv F_\delta \partial_{v_\delta} f v_\alpha v_\beta v_\gamma = -n[&F_\alpha(\theta\delta_{\beta\gamma}+u_\beta u_\gamma)+F_\beta(\theta\delta_{\alpha\gamma}+u_\alpha u_\gamma)\\ &+F_\gamma(\theta\delta_{\alpha\beta}+u_\alpha u_\beta)]\end{aligned} \tag{6.45}$$

6.1.3.2 Taylor expansion

We obtain to second order Taylor expansion of the equation (**6.41**) to determine what the macroscopic equations are the Lattice Boltzmann equation simulates

$$\begin{aligned}&\partial_t f_i + v_{i\alpha}\partial_\alpha f_i + \frac{1}{2}[\partial_t(\partial_t f_i + v_{i\alpha}\partial_\alpha f_i)+\partial_\beta(\partial_t f_i v_{i\beta}+v_{i\beta}v_{i\alpha}\partial_\alpha f_i)]+F_i+O(\partial^3)\\ &=\frac{1}{\tau}(f_i^0-f_i)\end{aligned} \tag{6.46}$$

The equation is not the Boltzmann equation (**6.18**) that setted out to simulate because with second derivative there are lots of additional terms. In these additional terms there

is a discretization error because of the the simple discretization scheme. For now the equation can be writen as

$$f_i = f_i^0 - \tau(\partial_t f + v_{i\alpha}\partial_\alpha f_i + F_i) \tag{6.47}$$

to express the f_i in terms of the equilibrium distribution f_i^0 . With expressing all components in terms of the equilibrium distribution,

$$\begin{aligned}&\partial_t f_i^0 - \tau\partial_t(\partial_t f_i + v_{i\alpha}\partial_\alpha f_i + F_i) + v_{i\alpha}\partial_\alpha f_i^0 + \partial_\alpha(\partial_t f_i^0 v_{i\alpha} + v_{i\alpha}v_{i\beta}\partial_\beta f_i^0 + F_i)\\ &+\frac{1}{2}[\partial_t(\partial_t f_i + v_{i\alpha}\partial_\alpha f_i) + \partial_\beta(\partial_t f_i^0 v_{i\beta} + v_{i\beta}v_{i\alpha}\partial_\alpha f_i^0)] + O(\partial^3) = \frac{1}{\tau}(f_i^0 - f_i)\end{aligned} \tag{6.48}$$

The discretization errors are of exactly the same form as the higher order terms for the expression of the distribution function in terms of the equilibrium distribution function. Now equation can be written as,

$$\begin{aligned}&\partial_t f_i^0 + v_{i\alpha}\partial_\alpha f_i + \left(\tau - \frac{1}{2}\right)[\partial_t(\partial_t f_i + v_{i\alpha}\partial_\alpha f_i) + \partial_\beta(\partial_t f_i^0 v_{i\beta} + v_{i\beta}v_{i\alpha}\partial_\alpha f_i^0)] + O(\partial^3)\\ &= \frac{1}{\tau}(f_i^0 - f_i)\end{aligned} \tag{6.49}$$

except the relaxation time is renormalized to be $\tau - 1/2$, the equation is the same equation which would be obtained for the Boltzmann equation. So if an equilibrium distribution is chosen with the appropriate moments, automatically the hydrodynamic equations can be simulated to the same order that derived the hydrodynamic limit.

6.1.3.3 One dimensional implementation

For the implementation an equilibrium distribution which fulfills the equivalent definitions of (**6.19**) - (**6.23**) must be defined

$$\sum_i f_i^0 = n, \tag{6.50}$$

$$\sum_i f_i^0(v_{i\alpha} - u_\alpha) = 0, \tag{6.51}$$

$$\sum_i f_i^0 (v_{i\alpha} - u_\alpha)(v_{i\beta} - u_\beta) = n\theta\delta_{\alpha\beta}, \tag{6.52}$$

$$\sum_i f_i^0 (v_{i\alpha} - u_\alpha)(v_{i\beta} - u_\beta)(v_{i\gamma} - u_\gamma) = 0, \tag{6.53}$$

$$\sum_i f_i^0 (v_{i\alpha} - u_\alpha)(v_{i\beta} - u_\beta)(v_i - u)^2 = n\theta^2\delta_{\alpha\beta} \tag{6.54}$$

where the difference between (**6.54**) and (**6.23**) is due to the fact that one dimensional model is considered instead of a three dimensional model. Five equations is required for one dimensional model. And a set of 5 velocities v_i and corresponding equilibrium distribution terms f_i^0 are required. If the symmetric velocity set is chosen,

$$\{v_i\} = \{-2c, -c, 0, c, 2c\} \tag{6.55}$$

the equilibrium distribution is obtained

$$f_0^0 = \frac{n(4c^4 + 3\theta^2 + 6\theta u^2 + u^4 - 5c^2(\theta + u^2))}{4c^4} \tag{6.56}$$

$$f_1^0 = \frac{n(-3\theta^2 + 4c^3u - 6\theta u^2 - u^4 + 4c^2(\theta + u^2) - c(3\theta u + u^3))}{6c^4} \tag{6.57}$$

$$f_{-1}^0 = \frac{n(-3\theta^2 - 4c^3u - 6\theta u^2 - u^4 + 4c^2(\theta + u^2) + c(3\theta u + u^3))}{6c^4} \tag{6.58}$$

$$f_2^0 = \frac{n(3\theta^2 - 2c^3u + 6\theta u^2 + u^4 - c^2(\theta + u^2) + 2c(3\theta u + u^3))}{24c^4} \tag{6.59}$$

$$f_{-2}^0 = \frac{n(3\theta^2 + 2c^3u + 6\theta u^2 + u^4 - c^2(\theta + u^2) - 2c(3\theta u + u^3))}{24c^4} \tag{6.60}$$

With these the actual implementation of the lattice Boltzmann method defined in (**6.41**) can be leaved.

6.1.3.4 Isothermal Lattice Boltzmann

Lattice Boltzmann simulations application area is mostly simulate the continuity and Navier Stokes equations. At these simulations temperature can be assumed as constant and instead it serves as a thermostat, the equilibrium distribution will no longer conserve energy. This condition removes the requirement for the equilibrium equations to fulfill equation (**6.54**). For the calculation of heat equations this moment was needed. For the full thermohydrodynamic model five velocities are needed. And one constraint can be dropped, so four velocity model to fulfill the remaining four constraints. For saving memory and cpu time the number of required velocities can be reduced. The determination of the temperature can be used as an additional degree of freedom. The four equation can be used to determine f_{-1}^0, $f_0^0 f_1$, and θ. This technique can work but θ must be a constant independent of n and u for our usual solution.

Using the D1Q3 velocity set $v_i = \{-1,0,1\}$ it is easy to see that (**6.50**) to (**6.52**) require

$$f_{-1}^0 = \frac{1}{2}n(-u+\theta+u^2) \tag{6.61}$$

$$f_0^0 = n(1-\theta-u^2) \tag{6.62}$$

$$f_1^0 = \frac{1}{2}n(u+\theta+u^2) \tag{6.63}$$

θ can be calculated from (**6.53**) with sing these solutions for the f_i^0 :

$$\theta = \frac{1}{3} - \frac{u^2}{3} \tag{6.64}$$

The velocity must be smaller than the lattice velocity $c = 1$ and also θ must be nearly constant. Lots of standard Lattice Boltzmann models use this smaller velocity sets. The third moment of the equilibrium distribution function can be modified for models in an arbitrary number of dimensions, as,

$$\sum_i f_i^0 (v_{i\alpha} - u_\alpha)(v_{i\beta} - u_\beta)(v_{i\gamma} - u_\gamma) = n u_\alpha u_\beta u_\gamma \tag{6.65}$$

and the term in u^3 can be neglected. If it is not negligible, this terms will lead to violations of Galilean invariance.

There are variety of velocity sets and corresponding equilibrium distributions with, depending on the dimensionality of the space you want to simulate, in the literature.

Equilibrium distribution can be given by:

$$f_i^0 = nw_i \left[1 + \frac{3}{c^2} u.v_i + \frac{9}{2c^4}(u.v_i)^2 - \frac{3}{2c^2} u.u\right] \tag{6.66}$$

The w_i's are weights depending on the set of velocities. The values for commonly used models are given below.

For D2Q9 the weights are:

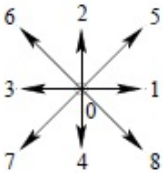

$$w_i = \begin{cases} 4/9 & i = 0 \\ 1/9 & i = 1,2,3,4 \\ 1/36 & i = 5,6,7,8 \end{cases} \tag{6.67}$$

For D3Q15 the weights are:

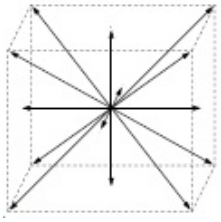

$$w_i = \begin{cases} 2/9 & i = 0 \\ 1/9 & i = 1-6 \\ 1/72 & i = 7-14 \end{cases} \tag{6.68}$$

For D3Q19 the weights are:

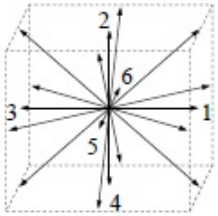

$$w_i = \begin{cases} 1/3 & i = 0 \\ 1/18 & i = 1-6 \\ 1/36 & i = 7-18 \end{cases} \tag{6.69}$$

For D3Q27 the weights are:

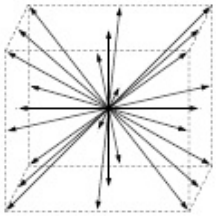

$$w_i = \begin{cases} 8/27 & i = 0 \\ 2/27 & i = 1-6 \\ 1/216 & i = 7-14 \\ 1/54 & i = 15-26 \end{cases} \tag{6.70}$$

Note: The moments of the equilibrium distribution function (**6.50**) to (**6.52**) and (**6.65**) are not sufficient to determine the w_i for large velocity sets. The weights to D3Q15 can be considered as a subset of D3Q27. The D3Q15 model weights can be recover from D3Q27 and moments can be still same.

6.1.3.5 Non-ideal fluids

As shown above, the Boltzmann equation leads to the Navier-Stokes equation for ideal systems, also we can use it for non-ideal systems too. For non-ideal systems Navier-Stokes equation can be given by

$$n\partial_t u_\alpha + n u_\beta \partial_\beta u_\alpha = -\partial_\beta P_{\alpha\beta} + \partial_\beta[\eta(\partial_\beta u_\alpha + \partial\alpha u_\beta - \frac{2}{3}\partial_\gamma u_\gamma \delta_{\alpha\beta})] \tag{6.71}$$

The non-ideal behaviour can be recovered by

$$nF_\alpha = -\partial_\beta(P_{\alpha\beta} - n\theta\delta_{\alpha\beta}) \tag{6.72}$$

for any given non-ideal pressure tensor $P_{\alpha\beta}$. These pressure tensors can be derived for an iso-thermal system from the system's free energy.

A forcing term F can be implemented by

$$F_i^0 = nw_i \left[\frac{3}{c^2} F_\alpha v_{i\alpha} + \frac{9}{2c^4} (F_\alpha u_\beta + F_\beta u_\alpha) v_{i\alpha} v_{i\beta} - \frac{3}{c^2} F_\alpha u_\alpha \right] \tag{6.73}$$

Note: There can be additional terms for the surface tension. Introducing a forcing of the form of (**6.72**) will lead to a surface tension.

6.1.3.6 Boundaries

In the fluid dynamics some boundaries must be implemented to the simulation. And usually non-slip boundary condition desired at those boundaries. For the implementation of a boundary the simplest way is drawing the boundary and marking all links which was cut by the boundary. On these links instead of free streaming the densities are bounced-back

$$f_i(x, t+1) = f_{-i}(x, t) \tag{6.74}$$

the velocity index $-i$ is defined as $v_{-i} = -v_i$. The effective boundary is at the middle of the between links.

If the boundary is moving, this boundary condition must be modified. For the modification a Galilean transformation of the distribution can be performed into the rest of the frame of boundary, the bounce-back operation can be performed, and then the flow back can be transformed into the original. A Galilean transform can be defined as

$$f'(v_i) = f_i(v_i) + G(v_i, U) \tag{6.75}$$

Then the moving bounce back boundary condition can be written as

$$f(v_i, t+1) = f'_{-i} + G(-v_i, -U) = f_{-i} + G(v_i, U) + G(-v_i, U) \tag{6.76}$$

The usual choice for the moments of the Galilean transformation

$$(G(v_i, U) + G(-v_i, -U)) = \frac{6}{c^2} w_i n U_\alpha v_{i\alpha} \tag{6.77}$$

The streaming step can be replaced for each density crossing the moving boundary

$$f_i(x,t+1) = f_{-i}(x,t) + \frac{6}{c^2} w_i n U_\alpha v_{i\alpha} \tag{6.78}$$

6.2 Discrete Element Method (DEM)

Discrete Element Method is one of the powerful numerical modeling method to model the kinematic and dynamic behaviours of discontinuous bodies (like RBC). These bodies can interact with each other through collisions. Today Discrete Element Method can simulate millions of particles on a single processor with progress of nearest neighbor sorting algorithms. This technique is finding a large area in the field of discontinuous engineering problems with its simulation power. In Discrete Element Method the forces acting on the discontinuous bodies (particles like RBC) are summed and the equations of motion of Newton and Euler are integrated to obtain the velocity and the position of the particles in the next time step.

The term discrete element methods will here be understood to comprise different techniques suitable for a simulation of dynamic behaviour of systems of multiple rigid, simply deformable (pseudo-rigid) or fully deformable separated bodies of simplified or arbitrary shapes, subject to continuous changes in the contact stares and varying contact forces, which in turn influence the subsequent movement of the bodies. Such problems are non-smooth in space (separate bodies) and in time (jumps in velocities upon collisions) and the unilateral constraints (non-penetrability) need to be considered. A system of bodies changes its position continuously under the action of external forces and interaction forces between bodies, which may eventually lead to a steady-state configuration, once static equilibrium is achieved. For rigid bodies, the contact interaction law is the only constitutive law considered, while the continuum constitutive law (e.g. elasticity, plasticity, damage, fracturing) needs to be included for deformable bodies.

Computational modelling of multi-body contacts (both the contact detection and contact resolution) represents the dominant feature in discrete element methods, as the number of bodies considered may be very large. If the number of potential contact surfaces is relatively small (e.g. non-linear finite element analysis of contact problems) it is convenient to define groups of nodes, segments or surfaces which belong to a possible

contact set a priori. These geometric attributes can then be continuously checked against one another and the kinematic resolution can be treated in a very rigorous manner. Bodies which are possibly in contact may be internally discretized by finite elements, and their material behaviour can essentially be of any complexity.

The category of discrete element methods specifically refers to simulations involving a large number of bodies where the contact locations and conditions cannot be defined in advance and need to be continuously updated as the solution progresses. Discrete element methods are most frequently applied to macroscopically discrete system of bodies (jointed rock, granular flow) but have also been successfully utilized in a microscopic setting, where very simple interaction laws between individual particles provide the material behaviour observed at a homogenized, macroscopic level.

The discrete element method is most commonly defined as a computational modelling framework which allows finite displacements and rotations of discrete bodies, including complete detachment and recognizes new contacts automatically, as the calculation progresses.

6.2.1 DEM formulations

The main formulation of the discrete element method, was based on deformable contacts of the rigid circular bodies in two dimensions. The general solution scheme was formulated in an explicit time-stepping format for the discrete element method. Particle movements are driven by external forces and some contact forces which are normal, tangential contact forces and viscous contact forces. The discrete element method considers that each particle in turn and at a definite time determines external or contact forces acting on it. For determining the particles movement during the next time step, the unbalanced forces considered.

The main computation progress of DEM is typically occurred by solving the given discrete element's equations of motion and updating the contact forces which was occurred by contacts between different particles or/and resulting from the boundaries (see Figure 6.1).

The RBSM (Rigid Bodies Spring Model) was proposed as a plastic analysis framework which has generalized limit (see Figure 6.2). And the solid structures were assumed as

assemblies of rigid blocks which was combined with deformable interfaces (normal and tangential springs).

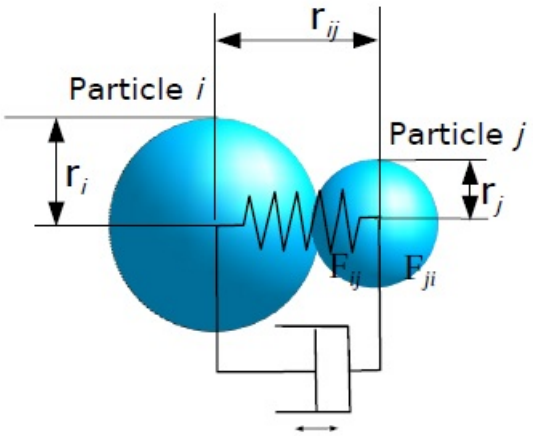

Figure 6.1: Discrete element particles (bodies) in contact.

The stiffness matrix was obtained by the related rigid particles are connected each others with distributed normal and tangential springs whose stiffness values are k_n, and k_s per unit length, respectively. The displacement field within an arbitrary two dimensional block is expressed based on a centroid displacement and rotation $(u, v, \theta)^T$.

In the Figure 6.2 the displacements at a common interface point P were defined independently as a centroid degree of freedoms $(u_i, v_i, \theta_i)^T$ and $(u_j, v_j, \theta_j)^T$ of the two neighbouring blocks with centroids located at (x_i^0, y_i^0) and (x_j^0, y_j^0), respectively.

$$
\begin{aligned}
&U_p = Q_p u \\
&U_p = \left[\begin{array}{cccc} U_p^i & ,V_p^i & ,U_p^j & ,V_p^j \end{array} \right]^T \\
&u = \left[\begin{array}{cccccc} u_i & v_i & \theta_i & u_j & v_j & \theta_j \end{array} \right]^T \\
&Q_p = \left[\begin{array}{cccccc} 1 & 0 & -(y_p - y_i^0) & 0 & 0 & 0 \\ 0 & 1 & (x_p - x_i^0) & 0 & 0 & 0 \\ 0 & 0 & 0 & 1 & 0 & -(y_p - y_i^0) \\ 0 & 0 & 0 & 0 & 1 & (x_p - x_i^0) \end{array} \right]
\end{aligned}
\tag{6.79}
$$

and the relative displacements at the location P,

$$
\delta_p = \left[\begin{array}{cc} \delta_n^P & \delta_s^P \end{array} \right]^T = M\tilde{U}_P = M\tilde{R}Q_P u = Bu \tag{6.80}
$$

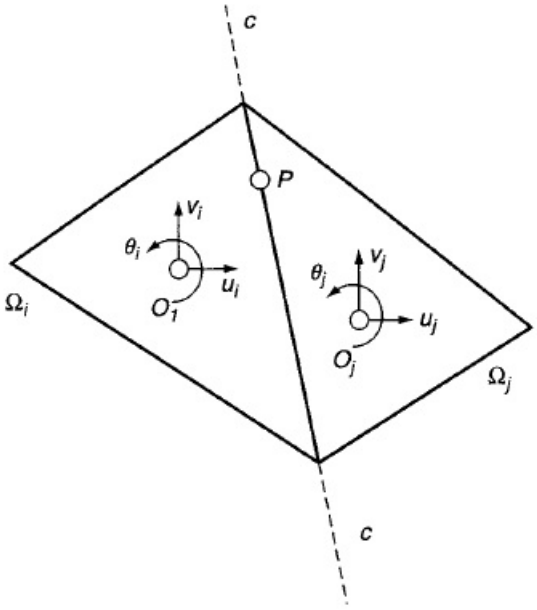

Figure 6.2: Two rigid blocks with an elastic interface contact in RBSM.

$$M = \begin{bmatrix} -1 & 0 & 1 & 0 \\ 0 & -1 & 0 & 1 \end{bmatrix} \text{ and } \tilde{U}_P = \tilde{R}U_P = \tilde{R}Q_P u \tag{6.81}$$

after U_P is projected to $\tilde{U}_P$ which was aligned to the local coordinate system along the interface. The constitutive relation in plane stress is expressed as,

$$\sigma = D\delta \quad \sigma = \begin{bmatrix} \sigma_n & , \tau_s \end{bmatrix}^T \tag{6.82}$$

$$D = \begin{bmatrix} k_n & 0 \\ 0 & k_s \end{bmatrix} \quad k_n = \frac{(1-\nu)E}{h(1-2\nu)(1+\nu)} \quad k_s = \frac{E}{h(1+\nu)} \tag{6.83}$$

where h is the total of shortest distances between the two block centroids of contact line. This approximate distance h is also used for the measurement of approximate normal and shear strain components with

$$\varepsilon_P = \begin{bmatrix} \varepsilon_n \\ \gamma_s \end{bmatrix}_P = \frac{1}{h}\begin{bmatrix} \delta_n \\ \delta_s \end{bmatrix} = \frac{1}{h}\delta_P \tag{6.84}$$

Applying the virtual work principle over the interface reveals,

$$f = \left[\int_S B^T DBds \right] u = Ku \tag{6.85}$$

The generalization of the method to the three dimensional form is straightforward. And the method can be interpretable as a finite element method with zero thickness interface elements. The only difference is the overall elastic behaviour is represented by the distributed stiffness springs along interfaces.

Because of some given criterion, the contact springs can be deactivated, so that the progressive failure can be modelled by widening discontinuities, through cracks and/or slippage at the interfaces.

Force Displacement Law

$$\begin{aligned}
&Relative\ Velocities:\ \dot{X}_i = (\dot{x}_i - \dot{y}_i) - (\dot{\theta}_x R_x + \dot{\theta}_y R_y) t_i \\
&Relative\ Displacements:\ \dot{n} = \dot{X}_i e_i, \dot{s} = \dot{X}_i t_i \\
&Contact\ Force\ Increments:\ \Delta n = n\Delta t, \Delta s = s\Delta t \\
&Total\ Forces:\ F_n = F_n^{n-1} + \Delta F_n, F_s = F_s^{n-1} + \Delta F_s \\
&Check\ For\ Slip:\ F_s = min(F_s, C + F_n tan\phi) \\
&Compute\ Moments:\ M_x = \sum F_x R_x, M_y = \sum F_y R_y
\end{aligned} \tag{6.86}$$

Equations Of Motion

$$\begin{aligned}
&Assume\ Force\ And\ Moment\ Constant\ Over\ \Delta t:\ \Delta t = (t^{n+1/2} - t^{n-1/2}) \\
&Acceleration:\ m\ddot{x}_i = \sum F_i, I\ddot{\theta} = M_i \\
&Velocity:\ \dot{x}_i^{n+1/2} = \dot{x}_i^{n-1/2} + \ddot{x}_i \Delta t, \dot{\theta}_i^{n+1/2} = \dot{\theta}_i^{n-1/2} + \ddot{\theta}_i \Delta t \\
&Assume\ Velocities\ Constant\ Over\ \Delta t:\ \Delta t = (t^{n+1} - t^n) \\
&Displacements:\ x_i^{n+1} = x_i^n + \dot{x}_i^{n+1/2} \Delta t \\
&Rotation:\ \theta^{n+1} = \theta^n + \dot{\theta}^{n+1/2} \Delta t
\end{aligned} \tag{6.87}$$

6.2.2 Contact detection

Discrete element method's principle algorithmic case is the detection of the particles in contact followed by the calculation of the contact forces due to contact. Generally the contact detection case can be stated as contact finding or overlap of a definite colliding particles with a number of particles from a target set of N bodies in R^n space. The

contact detection strategies are related with geometric characterization and topological attributes of interacting particles. If the colliding particles are simple geometries (like circle or sphere) the algorithmic check for a possible overlap is quite simple. Also the tangential contact plane is so perceptible. Contact detection algorithms are based on body based search or space based search. Body based algorithm is searching only the space in the neighbour of the specified discrete element. On the other hand space based algorithm is purposing the total searching space into a number of overlapping windows.

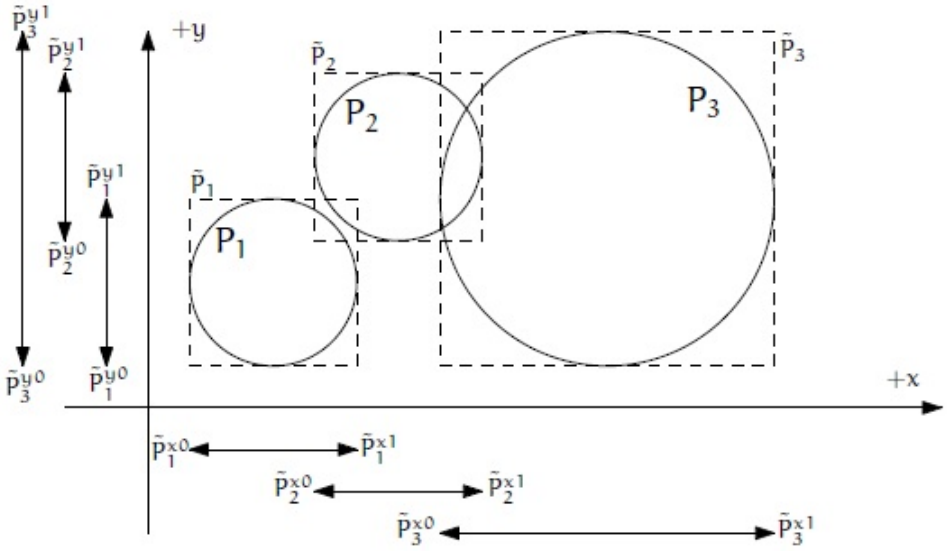

Figure 6.3: The sweep and prune algorithm used for collision detection.

For the calculation with arbitrary geometric shapes, mostly a two phased strategy is employed. The first step is that particles can be approximated by simpler geometric constructs. With this step the actual particle can be encircled and the possible contact pairs can be listed by a region search algorithm. Then followed by second step which is a detailed local contact resolution step.

For the detection of collision, efficient detection algorithms and powerful data representation concepts are taken from other disciplines, generally computer graphics, to describe the geometric position of a particle with data representation techniques. Also the decomposition of the computation space and various cell data representation for collision particles are adopted too. The issues of algorithm and data structures are quite involved and the relationship between the number of cells and the total number of particles is non linear.

For simple shapes very efficient data structures map a minimum set of parameters which uniquely define a domain in R_n into a representative point in an associated R_{2n} space (Fig.6.4)- for example, a one-dimensional segment $(a-b)$ is mapped into a representative point in two-dimensional space, with coordinates (a,b), or a two-dimensional rectangle of a size $(x_{min}-x_{max})$ and $(y_{min}-y_{max})$ is mapped to a representative point in a four-dimensional space $(x_{min},y_{min},x_{max},y_{max})$. Alternative representation schemes are also possible, e.g. by characterizing a rectangular domain in R^2 by the starting point coordinates (x_{min},y_{min}) and the two rectangle sizes (h_x,h_y) followed by a mapping into an associated R 4 space $(x_{min},y_{min},h_x,h_y)$. As the representation of the physical domain is reduced to a point, region search algorithms are more efficient in the mapped R_{2n} spaces than in the physical R_n space.

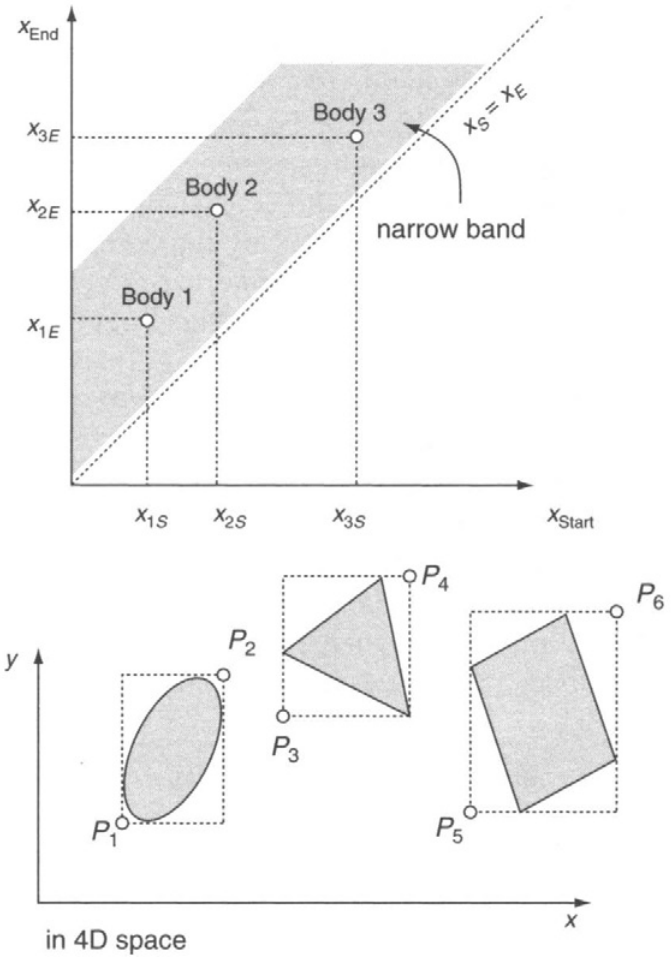

Figure 6.4: Mapping of a segment from one-dimensional space into a point in an associated two-dimensional space and mapping of a box in two dimensions into an associated four-dimensional space.

After listing the potential contact pairs, a exhaustive contact resolution algorithm is required. For this algorithm the particle geometries must be defined in detail. During

the contact resolution step, potential pairs is searched by the algorithm and if a contact is established, the alorithm must define the contact plane's orientation. Thus a local coordinate system (n,t,s) can be determined and the sliding or impenetrability conditions can be applied.

The particle geometry characterization can be categorized into three main groups:
1- Polygon or polyhedron representation,
2- Implicit continuous function representation,
3- Discrete function representation (DFR).

In two dimension the polygonal representation defines a particle in terms of corners and edges. And some algorithms can determine the intersection of two polygons. When the corner to edge or edge to edge contact is considered, the orientation of the contact plane can be defined easily.

Another possible procedure utilizes an optimum triangulation of the space between the polygons, whereby a collapse of a triangle indicates an occurrence of contact.

A continuous implicit function representation of bodies, provides an opportunity to employ a simple analytical check to identify whether a given point lies inside or on the boundary $(\phi(x,y) \leq 0)$ or outside $(\phi(x,y) > 0)$ of the body where

$$\phi(x,y) = \left(\frac{x}{a}\right)^{\beta_1} + \left(\frac{y}{b}\right)^{\beta_2} - 1 \qquad \textbf{(6.88)}$$

Unlike a polygonal representation, a complete intersection of overlapping superquadrics can be solved very difficultly. Because of the difficulties to find a solution the surfaces can be discretized to facets and nodes and the contact of a specific node on the particle can be found by inside-outside analytical check with respect to the functional representation of the other body.

Discrete Functional Representation (DFR) is a scheme for describing the particles boundary with a parametric function in one parameter. DFR is an algorithmic look-up table for replacing the continuous implicit function representation of bodies by the set of pre-evaluated function values on a background grid for the inside-outside check. The DFR concept in contact detection is illustrated through the polar DFR descriptor in two dimensions where, following the global region search for possible neighbours, the local contact is established by transforming the local coordinates of the approaching comer P_i

of a body i into the polar coordinates of the other body P_i^j and checking if an intersection between the segments $\overline{(O_j P_i^j)}$ and $\overline{(M_j N_j)}$ can be found.

6.2.3 Boundary conditions

In discrete element method boundaries can be defined at space level or at particle level. Space level boundaries are generally periodic boundaries. In periodic boundaries particles leaves the periodic cell on one side enter on the other side (see Figure 6.5). Also for periodicity the cell must be parallel piped shaped. Through the periodic boundary, the boundary related distortions can be eliminated. On the other hand particle level boundaries can be defined as fixing some particles in space. Other boundaries, which aim at a more faithful representation of experimental setups, might be flexible where a chain of particles is tied together by links or hydrostatic where forces corresponding to constant hydrostatic stress are exerted on particles on the boundary.

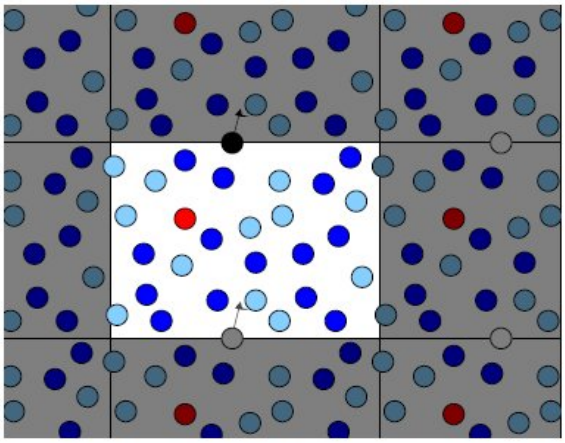

Figure 6.5: Schematic diagram of a simulation box with periodic boundary conditions.

7. COUPLING LBM AND DEM

Coupling LBM and DEM requires clarification of particle - fluid interaction mechanism. At this point interaction mechanism is related to boundary conditions, solid particle properties and solid - fluid area fractions. The required approach has to answer all of these points for a complete solution. Therefore our methodology is including a moving boundary approach using solid - fluid area fractions with viscoelastic particle collisions. In this study, we adopt a scheme proposed by Noble and Torczynski [1]. In this scheme, the collision operator in the LBM equation is modified by the solid area fraction γ in each nodal cell (see Feng et al. [13]).

The new BGK streaming and collision function:

$$f_i(x+e_i\Delta t, t+\Delta t) = f_i(x,t) - \frac{1}{\tau}(1-\beta)\left[f_i(x,t) - f_i^{eq}(x,t)\right] + \beta f_i^m \tag{7.1}$$

where β is a weighting function that depends on the solid area fraction γ in each nodal cell:

$$\int \beta = \gamma \tag{7.2}$$

f_i^m is a new collision term that accounts for the bounce- back of the non-equilibrium part of the distribution function and is given by

$$f_i^m = f_{-i}(x,t) - f_i(x,t) + f_i^{eq}(\rho, v_b) - f_{-i}^{eq}(\rho, v) \tag{7.3}$$

where - i denotes the direction opposite of i.

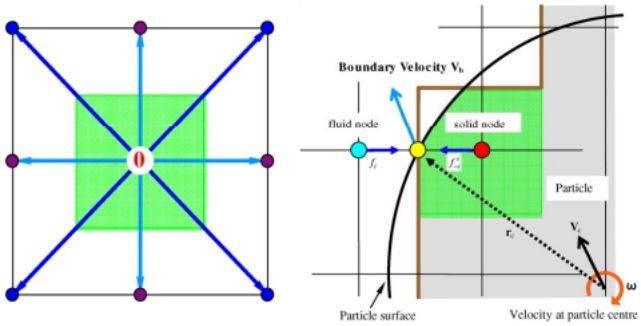

Figure 7.1: Noble and Torczynski's scheme (Ref [1]).

The hemodynamic forces and torque exerted on a particle can be computed as:

$$F_{fluid} = \frac{h^2}{\Delta t}\left[\sum_n \left(\beta_n \sum_i f_i^m e_i\right)\right] \tag{7.4}$$

$$T_{fluid} = \frac{h^2}{\Delta t}\left[\sum_n (x_n - x_c)\, x \sum_n \left(\beta_n \sum_i f_i^m e_i\right)\right] \tag{7.5}$$

where n is the number of nodes covered by a particle.

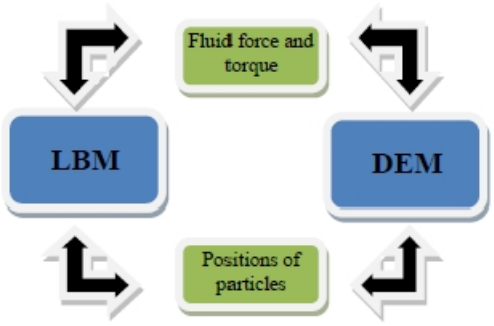

Figure 7.2: LBM - DEM coupling steps.

The coupling steps for LBM and DEM are described as:

- Step1: Calculate the fluid forces and torques with LBM.
- Step2: Send forces and torques to the DEM.
- Step3: Calculate the collisions and new positions of particles.
- Step4: Send the positions of particles to LBM.
- Step5: Go to Step1 and do first 4 steps again.

8. RESULTS

8.1 The Simulation of Thrombus Formation

In this simulation we have 2D vessel geometry with a fatty core area (see Fig. 8.1). The simulation was based on Newtonian blood plasma flows and the velocity profile is Poiseuille which is initialized with zero, and converges only slowly to the expected parabola. In the simulation, the artery flow was characterized by Poiseuille flow.

In order to modeling RBC aggregation, we used discrete particles. To simplify the idea, we choose circle model for RBCs with random initial positions.

The resulting thrombus formation is seen in Figure 8.1.

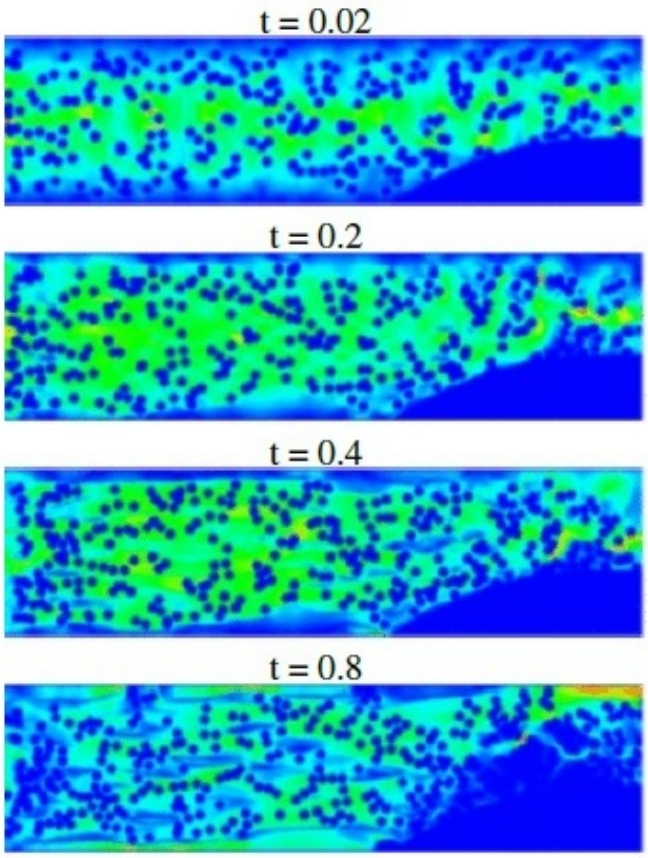

Figure 8.1: Results from thrombosis simulation.

Figure 8.1 shows that RBCs were aggregated at the diseased area because of the clotting force. When a particle entered diseased area, it will be under the influence of fluid forces and clotting forces. Therefore the effects of forces over the particle are computed by DEM software. If the clotting force is higher than others, the particles (RBCs) aggregate in the region of interest. If this blood clot detaches itself form the point that is formed, there maybe a possibility to stacked within any of the main arteries of the heart. This condition can induce to heart attack, stroke, myocardial infarction and other vital complications.

The numbers of RBCs were aggregated at the interest area within a time period shorter than a minute. At the beginning of the simulation the percentage of the aggregating particles were 1.5% while 68% at the end of the 0.8 minute. These results showed us that at the end of the simulation fluid flow speed up in the narrowing vessels area and fluid forces became dominant to clotting forces.

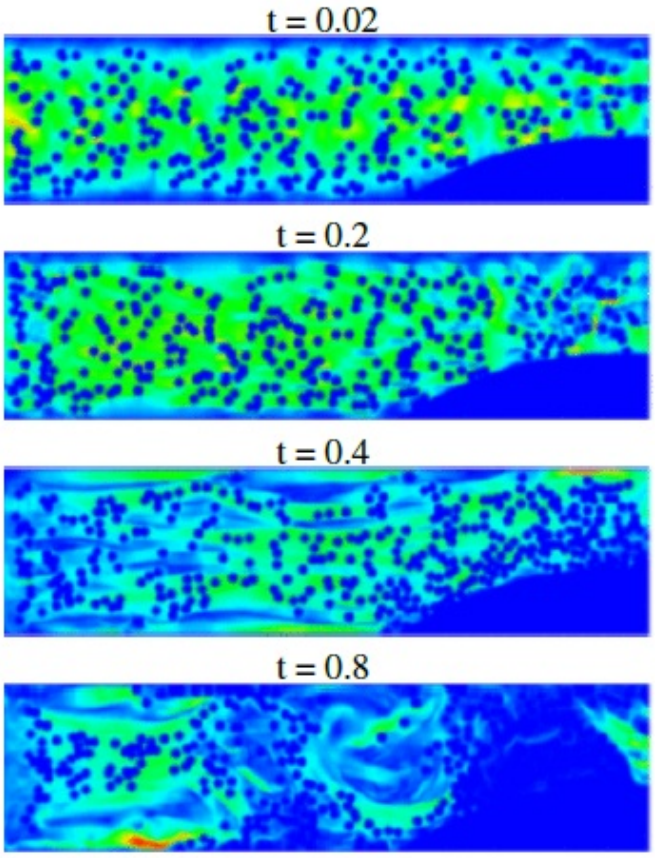

Figure 8.2: Results from thrombosis simulation (Clotting force is 2 times higher than Figure 8.1).

As we can see from the Figure 8.2, with the clotting force's increasing effects, more RBCs were aggregated at the diseased area. As a result of that, we can change the amount of aggregation with the clotting force effects.

Moreover, as we know the zymases concentration has special importance because of the effects on the clotting mechanism. To simulate these effects by changing the magnitude of clotting force, we can simulate different levels of zymases' effects. This technique provided us to simulate different clotting mechanisms with different zymases' effects comparatively.

9. DISCUSSION AND CONCLUSION

Due to the blood coagulation disorders are vital diseases, they must be understood carefully. To understand these diseases deeply, we can get assistance from computational simulations. As we discussed at the previous chapters we must simulate the blood coagulation process with different ways. For understanding the proteins and zymases' contributions to this process, we must simulate the whole biochemical system about the blood coagulation. Also for understanding the mechanical conditions of blood coagulation, we must simulate these processes with a biomechanical perspective.

In this study, our aim was to develop a base system for the simulation of blood coagulation process. We focused to develop a simulation for the flow of blood plasma and blood cells together. So we choose two new and powerful modeling technique together. For the simulation of blood flow, we choose Lattice Boltzmann Method and for the simulation of blood cells interactions, we choose Discrete Element Method together.

At the development stage of the blood coagulation simulation, we coupled these two methods (LBM and DEM). In the literature these coupling techniques are so new and can be developed for more realistic results. We adopt a scheme proposed by Noble and Torczynski [1].

After the completion of theoretical coupling steps of these two methods, we used two powerful library for making simulations in the computing environment (Palabos [18] and Yade [19]). After some benchmarking simulations, we developed a simulation for the most important disease of blood coagulation system, which is named as thrombosis.

At the thrombus formation simulations, we used red blood cells for the aggregation. And also for this aggregation, we create a clotting force with the help of the central force field technique. This force was supplanted for zymase's effects. When the particle enters the area of aggregation, they were influenced by a central force. The particles, which are under the influence of fluid drag force is lower than clotting force, were aggregate at the clotting area. As a result of this technique a thrombus formation occurred at the diseased area.

As we can see from the Results Chapter, we can change this thrombus' quantity through the clotting force effects. So with this relativity, the concentrations of zymases and production rates of zymases can be affected to the simulation through the help of this clotting force.

Our future plan for this study is create a simulation for blood coagulation with both biochemical and biomechanical perspective. So we will bond the concentrations and production rates of zymases with the clotting force for more realistic simulations. According to this view, we can predict that how can zymase paucity effects or how can mechanical conditions effects to the coagulation system, comparatively.

REFERENCES

[1] **Noble, D. and Torczynski, J.**, 1998. A lattice Boltzmann method for partially saturated computational cells, *International Journal of Modern Physics*, 1189–1201.

[2] **Tyurin, K.V. and Khanin, M.A.**, 2006. Hemostasis as an optimal system, *Mathematical Biosciences*, 167–184.

[3] **Hockina, M.F.**, **Jones, K.C.**, **Everse, S.J. and Mann, K.G.**, 2002. A Model for the Stoichiometric Regulation of Blood Coagulation, *The Journal of Biological Chemistry*.

[4] **Xu, C.**, **Zeng, Y.J. and Gregersen, H.**, 2002. Dynamic model of the role of platelets in the blood coagulation system, *Medical Engineering and Physics*, 587–593.

[5] **Bernsdorfa, J.**, **Harrison, S.E.**, **Smith, S.M.**, **Lawford, P.V. and Hose, D.R.**, 2006. Numerical simulation of clotting processes: A lattice Boltzmann application in medical physics, *Mathematics and Computers in Simulation*, 89–92.

[6] **Narracott, A.**, **Lawford, P.**, **Himeno, R. and Griffiths, P.**, 2005. Development and validation of models for the investigation of blood clotting in idealized stenoses and cerebral aneurysms, *The Japanese Society for Artificial Organs*, 56–62.

[7] **Sukop, M.C. and Thorne, D.T.**, 2006. Lattice Boltzmann Modeling. An Introduction for Geoscientists and Engineers, Springer-Verlag, New York.

[8] **Wagner, A.J.**, 2008. A Practical Introduction to the Lattice Boltzmann Method, North Dakota State University, Fargo.

[9] **Bernsdorf, J.M.**, 2008. Simulation of Complex Flows and Multi-Physics with the Lattice-Boltzmann Method, Ph.D. thesis, University of Amsterdam.

[10] **Cundall, P.A. and Hart, R.D.**, 1993. Numerical modelling of discontinua, *Comprehensive Rock Engineering*, 231–243.

[11] **Zienkiewicz, O. and Taylor, R.**, 2005. The Finite Element Method for Solid and Structural Mechanics, Elsevier, Oxford.

[12] **Munjiza, A.**, 2004. The Combined Finite-Discrete Element Method, John Wiley and Sons Ltd, West Sussex.

[13] **Feng, Y.T.**, **Han, K. and Owen, D.R.J.**, 2007. Coupled lattice Boltzmann method and discrete element modelling of particle transport in turbulent fluid flows: Computational issues, *International Journal for Numerical Methods in Engineering*, 1111–1134.

[14] **Shapiro, A.D.**, 2001. An Overview of Thrombophilia, *Hemaware*, 13–16.

[15] **Turkeri, H. and Çelebi, M.S.**, 2010. Non-Newtonian Blood Flow Simulation in a Realistic Artery Domain, *Fifth European Conference on Computational Fluid Dynamics ECCOMAS*.

[16] **White, F.M.**, 1991. Viscous Fluid Flow, McGraw-Hill, Inc., New York.

[17] **Qian, Y.H. and Lallemand, P.**, 1992. Lattice BGK Models for Navier-Stokes Equation, *Europhys. Lett.*, 479–484.

[18] Palabos: Parallel Lattice Boltzmann solver, *http://www.lbmethod.org/palabos/*.

[19] Yade: Open source discrete element method, *http://yade-dem.org/*.

CURRICULUM VITAE

Candidate's full name: Okan DOĞRU

Place and date of birth: İzmit, 1985

Permanent Address: İTÜ, Bilişim Enstitüsü, Ayazağa Kampüsü, 34469, Maslak, İstanbul

Universities and Colleges attended: Yıldız Technical University, Mechanical Engineering, 2008

Publications:

- **Doğru O.**, Çelebi M.S., Şaylan B., 2011: Computational Modeling of Thrombus Formation with Coupled Lattice Boltzmann and Discrete Element Methods, *IASTED (Biomed 2011) Proceedings, DOI:10.2316/P.2011.723-119, pp.145-150.*